DOI:10.14753/SE.2023.2903

PHOSPHORYLATION-DEPENDENT REGULATION OF THE RAC-SPECIFIC GTPASE ACTIVATING PROTEIN ARHGAP25

Ph.D. thesis

Éva Wisniewski, M.D.

Molecular Medicine Doctoral School

Semmelweis University

Supervisors: Roland Csépányi-Kömi, Ph.D.
Erzsébet Ligeti, M.D., Ph.D., D.Sc.

Official reviewers: Gábor Bőgel, M.D., Ph.D.
Imre Gombos, Ph.D.

Head of the Final Examination Committee:
Miklós Csala, M.D., Ph.D., D.Sc.

Members of the Final Examination Committee:
Sára Tóth, Ph.D.
Gabriella Sármay, Ph.D., D.Sc.

Budapest
2023

DOI:10.14753/SE.2023.2903

TABLE OF CONTENTS

DOI:10.14753/SE.2023.2903

DOI:10.14753/SE.2023.2903

DOI:10.14753/SE.2023.2903

1. LIST OF ABBREVIATIONS

AOS	Adams-Oliver Syndrome
ARMS	alveolar rhabdomyosarcoma
BRET	bioluminescence resonance energy transfer
CC	coiled coil
CFP	cyan fluorescent protein
CRC	colorectal cancer
CRIB	Cdc42/Rac-interactive binding motif
DLC1	Deleted in Liver Cancer 1
DTT	dithiothreitol
EGF	epidermal growth factor
ERK1	extracellular signal-regulated kinase 1
EST	expressed sequence tag
f-actin	filamentary actin
FI	fluorescence intensity
FLAIR	fluorescent activation indicator for Rho proteins
fMLP	N-formylmethionyl-leucyl-phenylalanine
FP	fluorescence polarization
FRET	Förster/Fluorescence resonance energy transfer
GAP	GTPase activating protein
GDI	guanine nucleotide dissociation inhibitor
GDP	guanosine 5′-diphosphate
GDPβS	guanosine 5′-[β-thio]diphosphate

GEF	guanine nucleotide exchange factor
GFP	green fluorescent protein
GSK-3	glycogen synthase kinase-3
GST	glutathione-S-transferase
GTP	guanosine-5'-triphosphate
GTPγS	guanosine 5'-[γ-thio]triphosphate
HI	heat-inactivated
HPSC	hematopoietic stem and progenitor cell
IGF	insulin-like growth factor
IPTG	isopropyl 1-thio-β-d-galactopyranoside
LPP	lambda protein phosphatase
MANT	2’(3’)-O-N-Methylanthraniloyl
MS	mass spectrometry
NADPH	Nicotinamide adenine dinucleotide phosphate
Nox	NADPH oxidase
NSCLC	non-small cell lung carcinoma
OPZ	opsonized zymosan
PAK	p21-activated kinase
PBD	p21-binding domain
PH	pleckstrin homology (domain)
PI3K	phosphoinositide 3-kinase
PKC	protein kinase C
PMA	phorbol 12-myristate 13-acetate

PMSF	phenylmethylsulfonyl fluoride
Raichu	Ras and interacting protein chimeric unit
RBD	Ras-binding domain
RLuc	*Renilla* luciferase
ROCK	Rho-associated protein kinase
ROS	reactive oxygen species
RSK1	ribosomal S6 kinase 1
SDS-PAGE	sodium dodecyl-sulfate polyacrylamide gel electrophoresis
smg	small G protein
TNFα	tumor necrosis factor alpha
TR-FRET	Time-Resolved Förster Resonance Energy Transfer
WASP	Wiskott Aldrich Syndrome Protein
YFP	yellow fluorescent protein

DOI:10.14753/SE.2023.2903

2. INTRODUCTION

ARHGAP25 is a GTPase activating protein (GAP) that specifically modifies the activity of the small G protein Rac and the importance of which in several neutrophilic granulocyte functions was recently recognized. In my thesis, I characterize the regulation of ARHGAP25 by phosphorylation and describe the development of a novel real-time bioluminescence resonance energy transfer (BRET)-based assay for GAP activity measurement. Therefore, pertinent literary knowledge is presented below on small G proteins, their GTPase activating proteins, with particular emphasis on ARHGAP25, and finally, on the currently available techniques for GAP measurements.

2.1 Small G proteins and their regulation

2.1.1 Small G proteins

Small or monomeric G proteins (also known as small GTPases) are important regulators of nearly all aspects of cellular processes, including but not restricted to cellular motion, shape change, polarity, survival and apoptosis, proliferation, differentiation, contact with neighboring cells and extracellular matrix, intracellular vesicular traffic, and transmembrane transport (1). Approximately 150 members of the superfamily have been identified, and they are structurally classified into five families: Ras, Rho, Rab, Arf, and Ran (2). They are composed of one polypeptide chain of ca. 20-30 kDa and have both GTP/GDP binding abilities as well as a GTPase activity. Functionally, they act as molecular switches, having two interconvertible forms: the GDP-bound inactive and GTP-bound active states. Upon activation, they release GDP and, given the intracellular GTP to GDP ratio (~10:1), bind GTP instead. This binding stabilizes the molecule and allows interaction with several downstream effectors. The GTP-bound form is converted to the inactive, GDP-bound form by their intrinsic GTPase activity, which is several orders of magnitude slower than that of the Gα subunit of the heterotrimeric G proteins (3).

Small GTPases have a very high affinity toward guanine nucleotides (GDP and GTP) with a K_d in the picomolar to nanomolar range (4). Thus, they are always present in a nucleotide-bound form and rarely in a nucleotide-free state (5). Therefore, to precisely operate the transition between states, they need regulatory proteins: the guanine

nucleotide exchange factors (GEFs), the GTPase activating proteins (GAPs), and the guanine nucleotide dissociation inhibitors (GDIs) – the latter influence only Rho and Rab family members (6) (***Figure 1***).

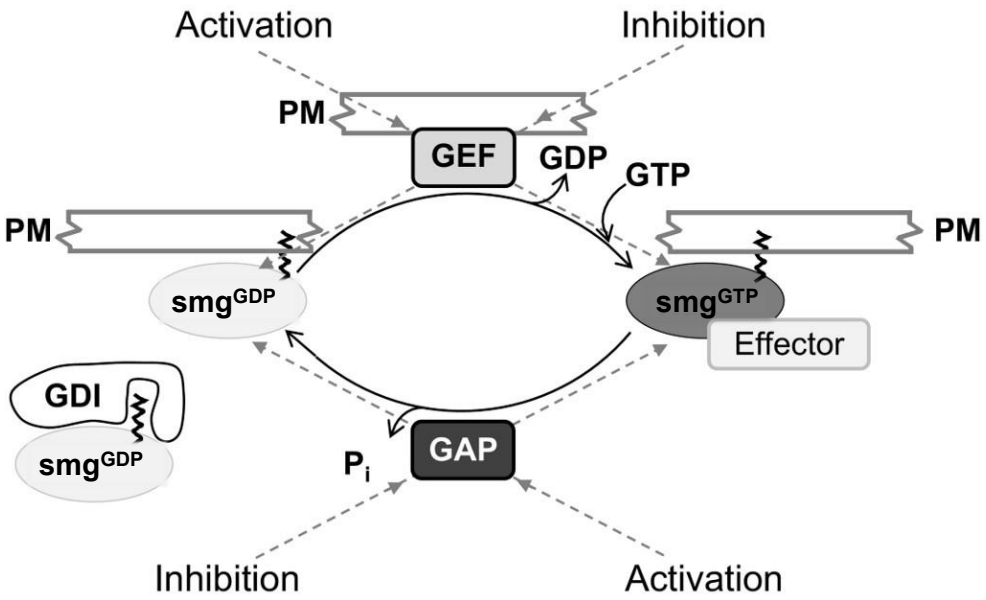

Figure 1. Regulation of the small G protein cycle. GEFs promote the activation of small G proteins, while GAPs are responsible for the inactivation. However, since both proteins can be activated and inhibited, they can eventually advance both the active and inactive state and, therefore, the effector functions (dashed arrows) (7). smg: small G protein, PM: phospholipid membrane, GTP: guanosine triphosphate, GDP: guanosine diphosphate, GEF: guanine nucleotide exchange factor, GAP: GTPase activating protein, GDI: guanine nucleotide dissociation inhibitor.

GEFs promote the release of GDP and the binding of GTP, considering the high GTP/GDP ratio within the cell (4). On the other hand, GAPs accelerate the slow endogenous GTP hydrolysis, resulting in the inactivation of the small G protein (8). At last, GDIs interact with the GDP-bound form and prevent nucleotide exchange. Furthermore, they can also remove their small G protein from the plasma membrane (where they usually operate) (1). All in all, the amount of active, GTP-bound small G protein and the continuation of signal transduction is always the result of the coordinated operation of these three regulatory proteins.

DOI:10.14753/SE.2023.2903

2.1.2 The molecular mechanism of the GTPase activating process

Small G proteins bind and hydrolyze nucleotides via their G domain, which contains five highly conserved regions (G1-G5) (9). Among them, the G2 and G3 regions, also called switch I and switch II regions, are essential for GTP binding and promoting the conformational switch. In the 'closed' GTP-bound form, there are two hydrogen bonds between γ-phosphate oxygens and the -NH_2 groups of threonine and glycine residues of the switch I and switch II regions (***Figure 2***). Their absence after hydrolysis allows the small G protein to relax into the 'open' GDP-bound conformation, thereby terminating the interaction with downstream effectors (10).

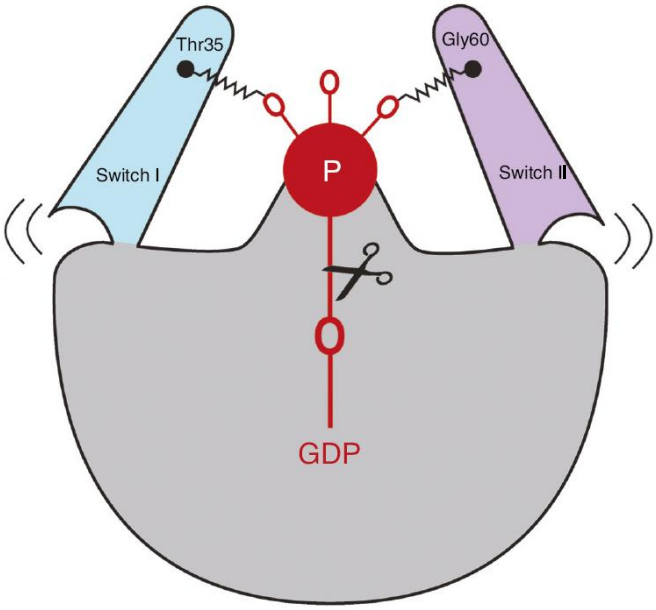

Figure 2. Schematic diagram of the Ras GTP-bound conformation with the conserved residues. Ras acts as a loaded spring: once the gamma-phosphate is hydrolyzed, switch I and switch II regions can take an open conformation (11). Thr35 and Gly60 refer to the threonine and glycine residues involved in GTP binding.

The endogenous GTP hydrolysis is very slow for nearly all small G proteins and therefore unsuitable for most signaling processes. However, GTPase activating proteins can catalyze this reaction by diverse mechanisms, first described in the case of Ras GTPase (12). First, they act by correctly positioning the attacking water molecule and stabilizing the water-positioning glutamine residue in the small G protein itself. Second, they interact with the phosphate-binding part of the small G protein and stabilize the transition state of

DOI:10.14753/SE.2023.2903

the hydrolysis reaction with their highly conserved arginine finger (***Figure 3***). GAPs of the Rho family – although structurally different from RasGAPs – act similarly (13). Naturally, family-specific variations of structural topology and catalytic mechanisms exist (14, 15) (***Figure 3***). Still, the amino acids involved in water molecule positioning and phosphate binding are evolutionarily conserved, and their mutations can result in the loss of catalytic activity (16).

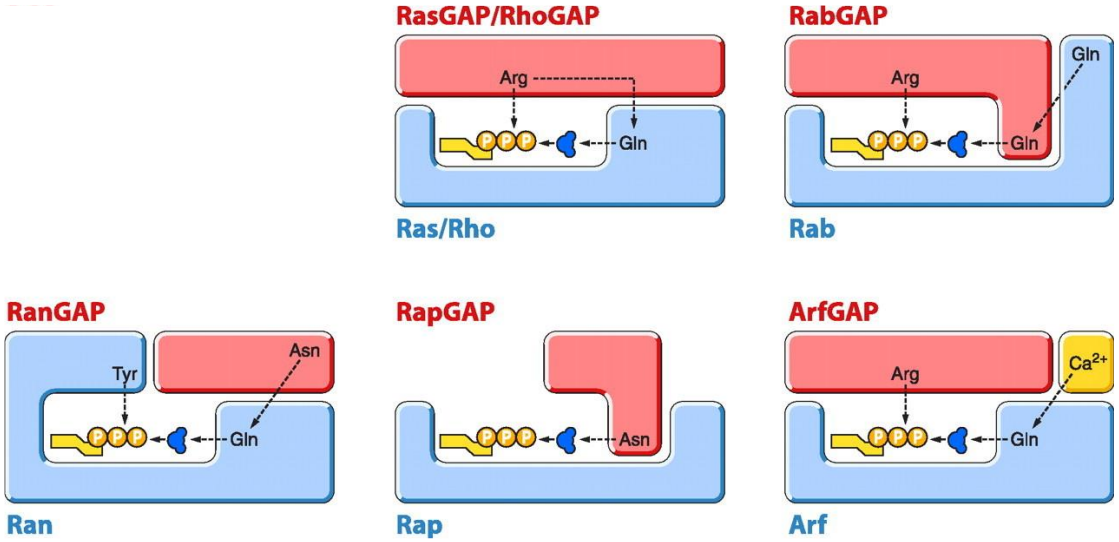

Figure 3. Mechanisms of the GAP-assisted GTP hydrolysis of small G proteins (8), modified by the author. The catalytic activity of small G proteins (light blue) binding GTP (yellow) and a water molecule (dark blue) can be accelerated by GAPs (red), primarily by stabilizing and positioning the interacting molecules.

2.1.3 Rho family GTPases and their GAPs

The Rho subfamily of small GTPases contains twenty members, among which the three best-studied members are RhoA, Rac1, and Cdc42 (17) (***Figure 4***).

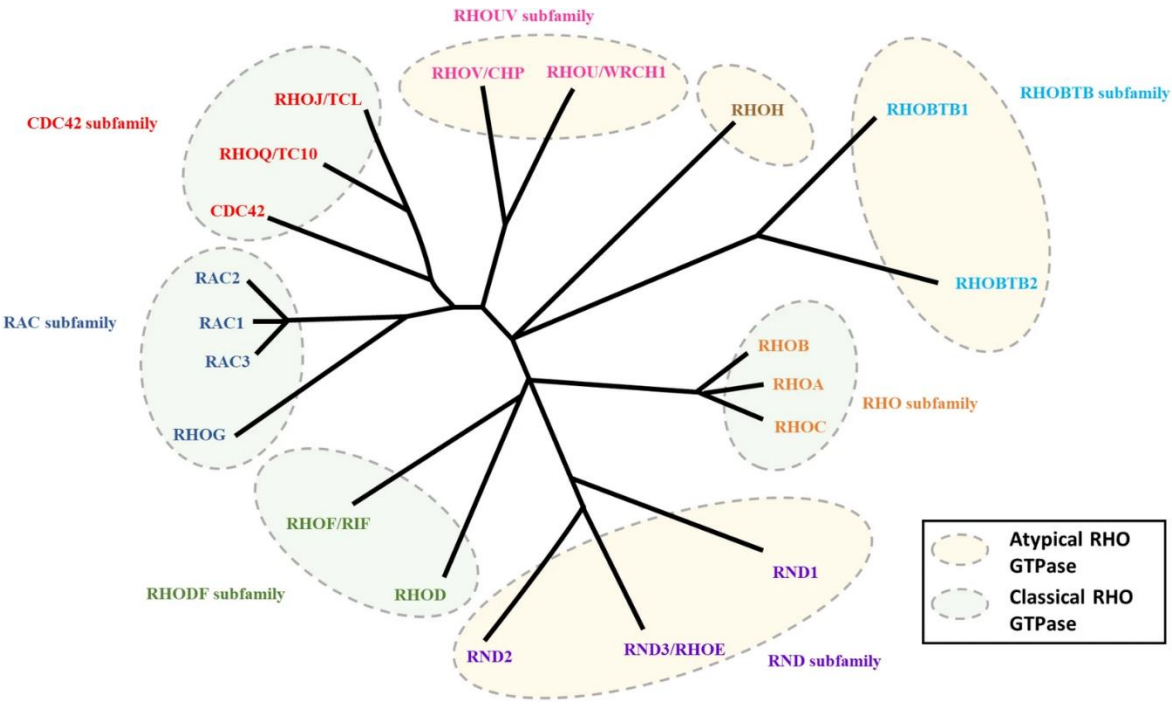

Figure 4. Phylogenetic tree of the Rho GTPase family (18).

The Rho family regulates actin-cytoskeleton reorganization, focal adhesions, cell movement, and immunological processes such as phagocytosis or production of reactive oxygen species (19-21). Therefore, they are particularly important in immune cells, such as neutrophilic granulocytes. The number of putative GAPs which regulate the Rho family GTPases is exceptionally high, 3-4-fold higher than the number of small G proteins (7, 22). These GAPs all contain a so-called GAP domain of approximately 20 kDa, which catalyzes the GTPase reaction of small G proteins, and many other interacting domains, enabling their strict temporal and spatial regulation (22) (***Figure 5***).

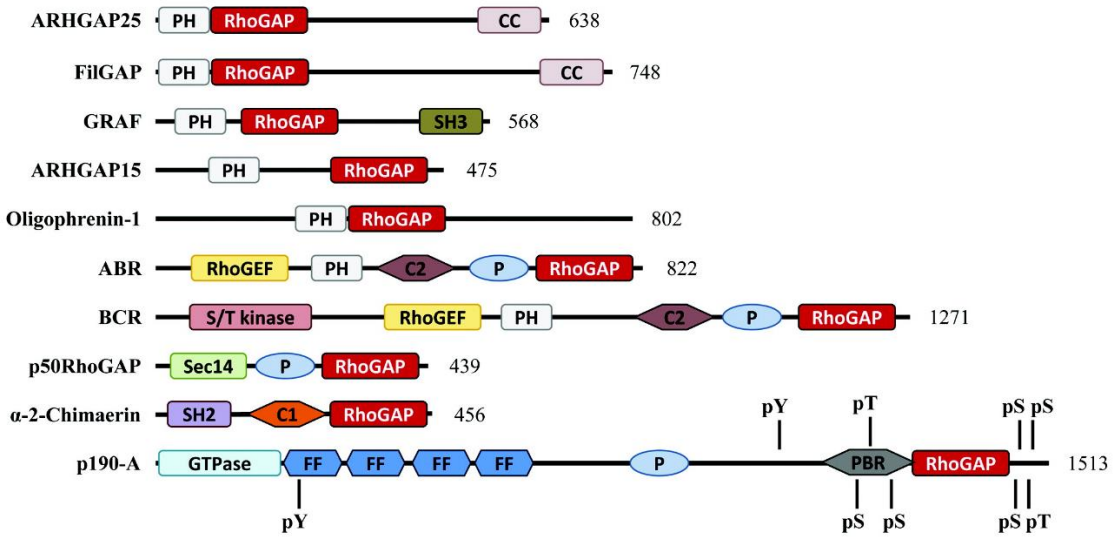

Figure 5. Diverse domain structure within the RhoGAP family (23). The GAP domain (in red) is responsible for the enzymatic GTPase activating effect. PH: pleckstrin homology domain; CC: coiled coil; SH3: Src Homology 3 domain; C2: calcium-dependent lipid binding domain; P: proline-rich domain; S/T kinase: serine/threonine kinase domain; Sec14: Sec14-like domain; SH2: Src Homology 2 domain; C1: cysteine-rich phorbol ester binding domain; FF: domains with two conserved phenylalanine residues; PBR: polybasic region.

The high number of GAPs acting on the Rho family GTPases raises the question of whether they are interchangeable, their effect is additive, or there are essential GAPs for each cell function/cell type. It seems that all the aforementioned scenarios are possible. Several pathological conditions are known where the absence of only one essential GAP leads to loss of function; for example, without p190ARhoGAP, aberrant neuronal morphogenesis can be observed (24). Similarly, loss of DLC1 (Deleted in Liver Cancer 1), a known tumor-suppressor, can cause overactivation of Rho and Cdc42, leading to uncontrolled cell growth and proliferation (25). Lőrincz *et al.* found that two Rac-specific GAPs, p50RhoGAP (ARHGAP1) and ARHGAP25 together regulate Nox2 activity, and their actions are additive (26). However, the same two GAPs have different effects on phagocytosis – ARHGAP25 overexpression significantly inhibits the rate of phagocytosis, while p50RhoGAP overexpression does not affect this process (7, 27).

Although GAPs were considered negative regulators for a long time, inhibiting an otherwise active GAP could be just as effective for small G protein activation as the GEF

pathway. Moreover, simultaneous activation of a GEF and inhibition of a GAP can result in a fulminant activation (7). In some cases, GEFs and GAPs even form regulatory complexes to maintain the optimal level of small G protein signaling (28).

2.1.4 The role of phosphorylation in Rho/Rac GAPs

Over 450 forms of post-translational modifications are responsible for regulating protein function and integrity, thereby increasing the complexity of the proteome within a cell (29). Among these modifications, phosphorylation is by far the most common, and approximately 30-50% of the proteome might be phosphorylated at a given time (30). The addition of a phosphate group to amino acid residues, such as serine, threonine, tyrosine – and less often histidine, aspartate, glutamate, lysine, arginine, and cysteine - can induce structural changes in proteins and thereby regulate essential cell functions, including signal transduction, cellular metabolism, cell growth and apoptosis (31, 32). On the other hand, phosphatases can remove the phosphate moiety, and both actions can activate or inactivate a protein.

A GAP's phosphorylation (or dephosphorylation) can directly affect the catalytic domain, altering its enzymatic activity. However, it is more common that phosphorylation on another part of the protein induces a change in localization, protein degradation, or protein-protein interactions, thereby indirectly affecting the GAP activity (33). In ***Table 1***, I summarized the remarkably diverse role of phosphorylation among GAPs of the Rho family.

Table 1. Diverse effects of phosphorylation in GAPs of the Rho family†.

GAP	Kinase	Effect of phosphorylation	Biological function	Reference(s)
MgcRacGAP	Aurora B	direct activation of GAP activity	cell division	(34, 35)
ARAP3	src family kinases	direct inhibition of GAP activity	cell spreading	(36)
p190BRhoGAP (ARHGAP5)	Insulin/IGF-1 receptor	binding to lipid rafts in the cell membrane	adipocyte differentiation	(37)
CdGAP (ARHGAP31)	ERK1/2, GSK-3	inhibition of GAP activity	vascular development, breast cancer cell migration and invasion	(38, 39)
CdGAP (ARHGAP31)	RSK	docking site formation for 14-3-3, intracellular sequestration	inhibition of cell rounding and migration	(40)
FilGAP	ROCK	release from the cytoskeleton	inhibition of lamellipodia formation and cell spreading	(41, 42)
p190ARhoGAP	PKCα	preventing phospholipid binding, changing substrate preference	RhoGAP activity increases, RacGAP activity decreases	(43)

†*Abbreviations: IGF: insulin-like growth factor, ERK: extracellular signal-related kinase, GSK-3: glycogen synthase kinase 3, RSK: ribosomal S6 kinase, ROCK: Rho-associated protein kinase, PKC: protein kinase C*

2.2 ARHGAP25, a Rac-specific GTPase with emerging importance

ARHGAP25, a GTPase activating protein, was first identified and characterized in an *in silico* study in 2004 (44). Not long after that, our research group was the first to clone it

from human peripheral blood cDNA and started examining its specificity, expression, function and regulation (27).

2.2.1 Structure and expression

ARHGAP25 was cloned from human peripheral blood cDNA resulting in a 646 amino acids long protein. The protein consists of three major domains: an N-terminal pleckstrin homology (PH) domain, a functionally active GAP domain, and a C-terminal coiled coil structure (***Figure 6***).

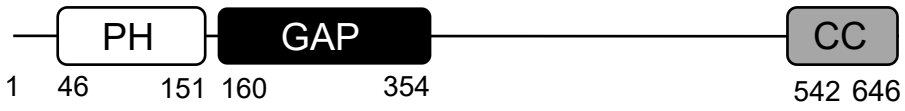

Figure 6. ARHGAP25's domain structure. PH: pleckstrin homology, GAP: GTPase activating protein (domain), CC: coiled coil.

Results of the expressed sequence tag (EST) database indicated its presence in hematopoietic cells and spleen, and our early experiments validated the expression in peripheral leukocytes at both mRNA and protein levels (27). However, in recent years, more and more papers have also reported on the expression of ARHGAP25 in non-hemopoietic tumor cells, where it plays a decisive role in tumorigenesis and metastasis (45-50).

2.2.2 Function

Like other members of the ARHGAP family, ARHGAP25 was suspected to be a GTPase activating protein for the Rho family GTPases based on *in silico* data. Our experiments showed that ARHGAP25 is a GAP acting on Rac but not on Rho or Cdc42 under *in vitro* conditions (27). Furthermore, inhibition of EGF-induced membrane ruffling, a Rac-dependent process by ARHGAP25 validated its RacGAP activity in COS-7 cells (27).

2.2.2.1 Function in leukocytes

Since ARHGAP25 was first thought to be a leukocyte-specific GAP, we started examining its function in hematopoietic cells. We showed that ARHGAP25 is a negative regulator of phagocytosis in COSphosFcγR and differentiated PLB-985 cell lines, as well as in primary macrophages (27). Schlam *et al.* confirmed that ARHGAP25 is essential in engulfing large particles by inhibiting Rac and enabling actin disassembly in RAW 264.7

macrophages (51). Both studies showed reduced f-actin accumulation and phagocytic impairment when ARHGAP25 was overexpressed.

ARHGAP25-silenced PLB-985 cells displayed significantly higher superoxide production upon opsonized zymosan activation, confirming its inhibitory role in ROS production as well (27). Using *Arhgap25*-deficient mice, our group identified ARHGAP25 as an important regulator in transendothelial migration (52).

Additionally, ARHGAP25 is essential for normal B cell development. *Arhgap25* deficiency in mice led to decreased peripheral blood B cell number as well as defects in B cell differentiation and germinal center formation. *Arhgap25*$^{-/-}$ B cells displayed increased motility both under basal conditions and upon CXCL12-driven chemotaxis (53). As a result, the phenotype of the mice is similar to the human WHIM syndrome (warts, hypogammaglobulinemia, infections, and myelokathexis) caused by an activating CXCR4 mutation and CXCL12 signaling upregulation.

2.2.2.2 Function in tumor cells

As stated above, ARHGAP25 is highly expressed in hematopoietic cells. However, ARHGAP25's role in many tumor types was confirmed, suggesting that its mutation, deficiency or overexpression can lead to changes in other cell types having low basal ARHGAP25 expression under physiological conditions. In fact, a growing number of evidence suggests a link between tumorigenesis and GAPs since the inactivation of GAPs can lead to continuous activation of small G protein-dependent signaling pathways, many of which are involved in cell proliferation (54).

ARHGAP25 can have both a negative and positive effect on tumor formation and metastasizing ability. For example, in a highly malignant pediatric tumor type, alveolar rhabdomyosarcoma (ARMS), the downregulation of RhoE and the subsequent activation of ROCK and ARHGAP25 enhance the invasive potential of ARMS cells (45). On the other hand, ARHGAP25 acts as a tumor suppressor in lung cancer cells: lower expression of ARHGAP25 was detected in human lung cancer cells. This study suggested that ARHGAP25 exerts its effect through the Wnt/β-catenin signaling pathway (46). Another study confirmed the negative correlation between ARHGAP25 expression and non-small cell lung carcinoma (NSCLC) malignancy and proposed a role in vasculogenic mimicry (47). Furthermore, ARHGAP25 was found to be downregulated in colorectal cancer (CRC), and the overexpression of the protein significantly inhibited CRC cell growth,

migration, and invasion, most likely through the Wnt/ β-catenin pathway (48, 49). A recent study also confirmed the role of ARHGAP25 in pancreatic adenocarcinoma, where ARHGAP25 acts as a tumor suppressor by inhibiting the AKT/mTOR pathway (50).

2.2.3 Regulation

As seen above, ARHGAP25 plays a diverse role in many cell types. However, we only know a little about its precise regulation and position in signaling pathways.

2.2.3.1 Regulation through gene expression

Although neutrophils are characterized by a short lifetime, regulation of ARHGAP25 through changes in expression level can be observed. Results from our workgroup showed that upon stimulation with opsonized bacteria, not only the mRNA but also the protein levels of ARHGAP25 decreased in 2 hours in human neutrophilic granulocytes (7). We propose that this drop in ARHGAP25 abundance can enhance Rac activity under physiological conditions where cytoskeleton rearrangement is necessary.

2.2.3.2 Regulation through protein-protein or protein-lipid interactions and changes in subcellular localization

ARHGAP25's domain structure enables it to interact with protein partners (by its coiled coil region) and specifically bind to lipid residues (by its PH domain), subsequently changing its intracellular localization. During phagocytosis, we observed the accumulation of ARHGAP25 around one side of the freshly formed phagosome. Interestingly, f-actin enrichment was seen on the opposing side as if their localization were mutually exclusive, suggesting the relevance of local Rac downregulation (7).

A comprehensive study by Schlam *et al*. investigated the role of Rho family GAPs in the phagocytosis of particles with different sizes (51). They showed that ARHGAP25, together with ARHGAP12 and SH3BP1 (SH3 Domain Binding Protein 1, a RhoGAP), was associated with the phagocytic cup in a PtdIns(3,4,5)P_3 - PI3K-dependent manner in RAW 264.7 macrophages (51).

2.2.3.3 Regulation through phosphorylation

Since phosphorylation is the most frequent post-translational modification, we suspected it plays a role in ARHGAP25's biological activity. Early experiments also suggested the

presence of phosphorylation when we observed a mobility shift in ARHGAP25's band in SDS-PAGE upon neutrophilic granulocyte activation (unpublished data, ***Figure 7***).

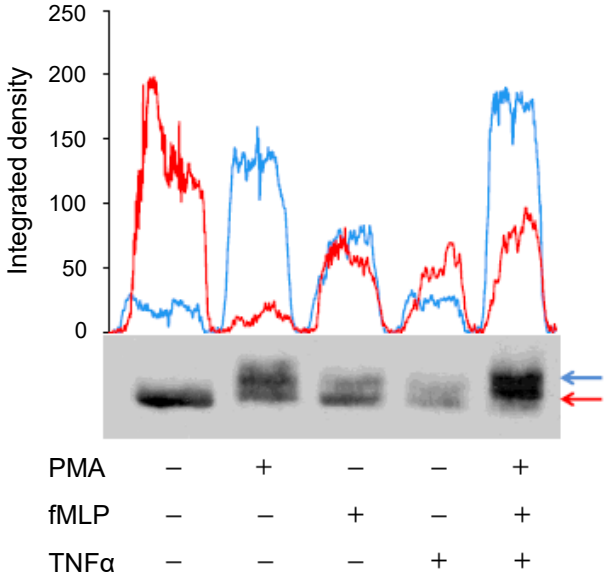

Figure 7. The mobility shift of ARHGAP25 following activation of neutrophilic granulocytes. Cells were treated with 100 nM phorbol 12-myristate 13-acetate (PMA), 20 ng/ml tumor necrosis factor-alpha (TNFα), and/or 1 µM N-formyl-methionyl-leucyl-phenylalanine (fMLP) for 5 minutes, then lysed and ran in SDS-PAGE. Blue and red arrows indicate the positions where the two densitometric measurements were taken along the blot.

The first functional data was only provided later, in collaboration with Wang *et al.* (55). Here, a newly developed phosphoproteomic analysis revealed highly different phosphorylation profiles of ARHGAP25 between resting and activated hematopoietic stem and progenitor cells (HSPCs). Furthermore, it was also shown that the mobilization of these cells from the bone marrow depended on the phosphorylation status of ARHGAP25 (55).

DOI:10.14753/SE.2023.2903

2.3 GAP activity measurements

Measuring both the intrinsic and GAP-stimulated GTPase activity of small G proteins is essential for delineating signaling pathways and characterizing GAP-GTPase interactions. However, the structural differences between GTP-bound and GDP-bound small G proteins are subtle and mainly limited to two small sections in the GTPase domain, the switch I and switch II regions (10). Therefore, it has been (and still is) considered a challenging task to develop a convenient assay for measuring GAP activity – one that is simple and cheap but at the same time robust and can be employed in high-throughput assays. In the following chapter, I would like to briefly discuss the currently available techniques for GTPase/GAP activity measurement, with particular emphasis on Rho family GAPs. The specific advantages and disadvantages of the methods will be systematically compared at the end of the section.

2.3.1 Methods based on guanine nucleotide labeling

2.3.1.1 Filter binding assay with radiolabeled guanine nucleotides

The radioisotope-based method was first described in the early ’90s and was considered a gold standard for a long time (3, 56). In this procedure, the small GTPase is ’loaded’ with GTP labeled on the gamma phosphate with ^{32}P (^{32}P-GTP). After stabilizing the binding with Mg^{2+}, the reaction starts by adding recombinant GAP protein to the sample. Aliquots are removed from the reaction at regular intervals and filtered through a 25 mm-diameter nitrocellulose membrane with a pore size of 0.45 μm. Thus, it is possible to separate the cleaved radiolabeled terminal phosphate group (in the flow-through) and the non-hydrolyzed GTP-GTPase complex, which, as a protein, strongly binds to the nitrocellulose membrane. The radioactivity of the membranes is measured, which is proportional to the level of intact GTP-bound small G protein. Therefore, it will be lower as the GAP activity rises (***Figure 8***).

DOI:10.14753/SE.2023.2903

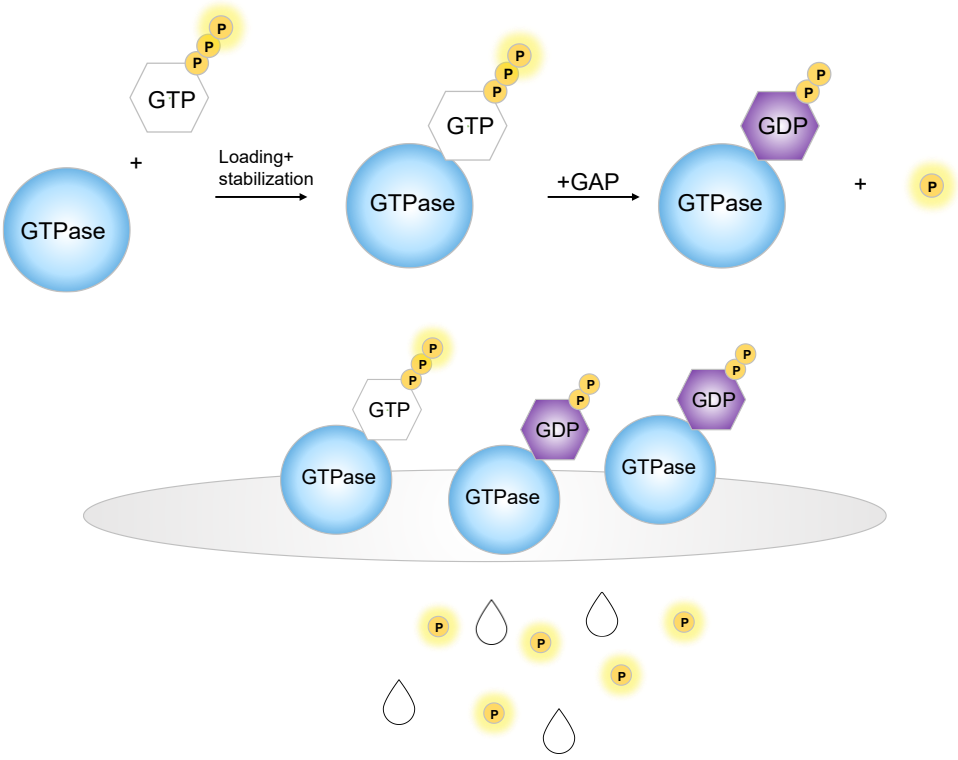

Figure 8. Schematic representation of the filter-binding GTPase assay. The small G protein contains a radiolabeled terminal phosphate in its GTP, which can be cleaved through its intrinsic or GAP-catalyzed GTPase reaction. Only the bound ^{32}P-GTP fraction stays on the membrane, and its radioactivity is proportional to the amount of the active small G protein remaining in the mixture.

2.3.1.2 Fluorescently labeled guanine nucleotides

Fluorescently labeled guanine nucleotides emerged as safer alternatives for monitoring nucleotide exchange. Since they allow continuous spectroscopic monitoring, a more detailed kinetic analysis can be performed (57). 2'(3')-O-N-methylanthraniloyl (mant) is the most widely used fluorescent molecule to label guanine nucleotides due to its small size and the fact that the emitted fluorescent signal increases dramatically upon binding to GTPases (58, 59). Typically, mant-labeling is used in GEF assays; the small G protein is loaded with mant-GDP, causing a high fluorescent signal, and as a GEF is added to the reaction, it catalyzes the dissociation of mant-GDP and the binding of GTP, decreasing the signal intensity (60, 61) (***Figure 9***).

DOI:10.14753/SE.2023.2903

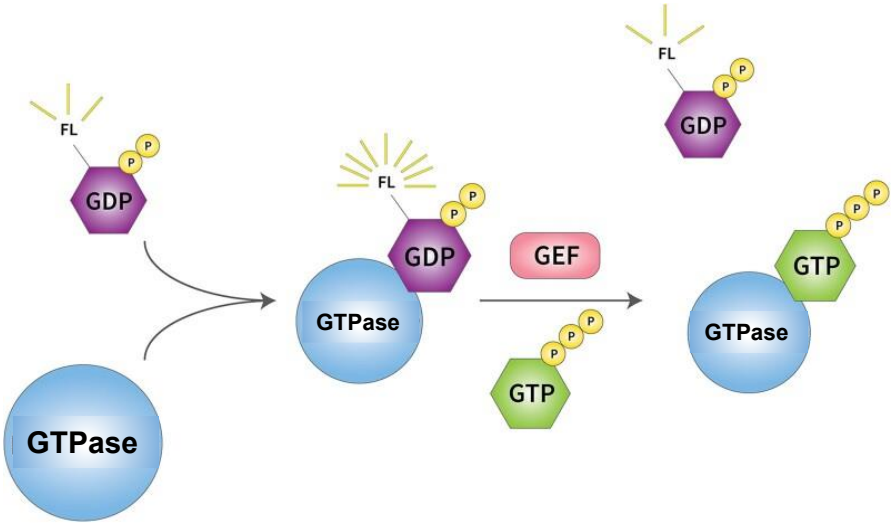

Figure 9. GEF activity assay utilizing fluorescently labeled GDP (62), modified by the author. The GTPases are loaded with the 2'(3')-O-N-methylanthraniloyl (mant)-GDP, which will be removed once GEFs are active and promote nucleotide exchange. The decrease in the fluorescent signal is proportional to GEF activity.

If the small GTPases are loaded with mant-GTP in advance, and GAPs are added to the reaction, we can also infer their activity from the decrease of the fluorescent signal (63-65). Unfortunately, recent evidence suggests that mant-GDP and mant-GTP can alter the kinetics of nucleotide hydrolysis and exchange of small G proteins and, therefore, their interaction with GEFs and GAPs (66). Moreover, the fluorescent signal upon small G protein binding is less intense in the case of some GTPases, especially Rho-family GTPases (67, 68). Therefore, recent studies suggest more effective alternatives over mant, such as the tamraGTP (68) or BODIPY-FL-guanine nucleotides (62).

2.3.2 High-throughput methods based on measuring the enzymatic products of the GTPase reaction

During GTP hydrolyzation, an inorganic phosphate and a GDP molecule are generated; all of these products can be used to measure the reaction's speed/biological activity. Methods utilizing the quantification of GTP, GDP, or P_i come mostly as commercially available assay kits in a convenient add-mix-read format and are ideal for high-throughput screenings.

2.3.2.1 GTPase-Glo™

Promega's (Madison, WI, USA) proprietary bioluminescent plate-based assay can measure the GTPase activity by detecting the remaining GTP after hydrolysis: the GTPase-Glo™ reagent converts GTP to ATP, which is converted to luminescence after adding the 'Detection Reagent' (***Figure 10***). With its design, the assay is able to measure both GEF and GAP activities (69).

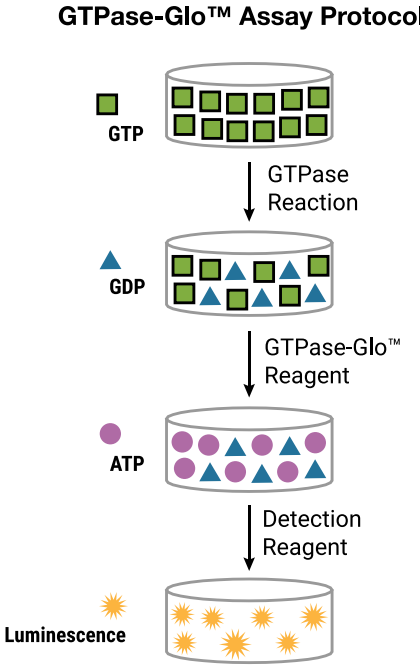

Figure 10. The GTPase-Glo assay converts the remaining amount of GTP to ATP, which is converted to a luminescent signal upon the addition of their detection reagent (70).

2.3.2.2 Transcreener® GDP Assay

This fluorimetric assay from BellBrook (Madison, WI, USA) determines GAP activity by measuring GDP production. The technology uses a specific GDP antibody and a far-red fluorescent tracer, and the produced GDP competes with the tracer, changing the fluorescent properties and providing fluorescent readout. Depending on the specific antibody, this robust assay is available with Fluorescent Polarization (FP), Fluorescence Intensity (FI), and Time-Resolved Förster Resonance Energy Transfer (TR-FRET) (***Figure 11***).

DOI:10.14753/SE.2023.2903

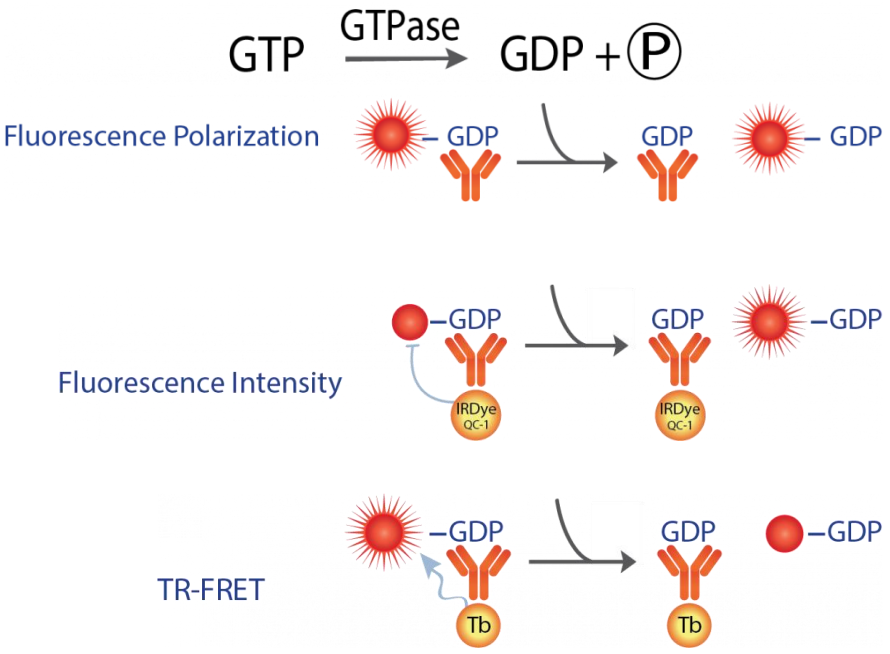

Figure 11: The Transcreener® GDP Assay from BellBrook takes advantage of a fluorescently labeled GDP-specific antibody that can be used in many fluorimetric assays (71). GTP: guanosine triphosphate, GDP: guanosine diphosphate, TR-FRET: Time-Resolved Förster Resonance Energy Transfer, Tb: terbium.

2.3.2.3 Phosphate detection

Measuring the inorganic phosphate (P_i) amount as a product of the GTPase reaction is a familiar idea; it was first mentioned in 1992 (72). The principle is simple: P_i reacts with a ribonucleoside, causing a shift in the absorbance maximum and enabling a spectrophotometric measurement. Since the measurement of P_i is an important output of all ATPase/GTPase reactions, almost all leading biotechnological companies introduced their own microplate-based phosphate assay kit (Invitrogen's (Waltham, MA, USA) EnzChek™, PiBlue™ from BioAssay Systems (Hayward, CA, USA), Abcam's (Cambridge, UK) colorimetric Phosphate Assay, *etc.*). The company Cytoskeleton (Denver, CO, USA) provides their version of the spectrophotometric assay with their so-called CytoPhos™ reagent. Moreover, their RhoGAP Assay contains relevant recombinant Rho family small G proteins and a RhoGAP as a positive control.

2.3.3 Methods based on specific binding

Small GTPases bind their downstream effectors with high affinity in their GTP-bound, active form. Thus, their specific interacting molecules are able to discriminate between

their inactive and active forms. Regarding the Rho family GTPases, these widely known effector proteins are Rhotekin and Rhophilin for Rho, p67Phox for Rac, and Wiskott Aldrich Syndrome Proteins (WASPs) and activated Cdc42-associated kinases (ACKs) for Cdc42 (73). The p21-activated kinases (PAKs) interact with both Cdc42 and Rac through their conserved region, which is known as Cdc42/Rac-interactive binding motif (CRIB). Interestingly, the CRIB motif alone (14 amino acids) is not enough for the high affinity binding, but a slightly larger, 44-amino acid region of PAK proved to be sufficient (74).

The following methods utilize the specific binding properties of these domains/structures.

2.3.3.1 Affinity precipitation

Affinity precipitation is mainly used in cell-based assays, where the GAPs may be exogenously expressed or suppressed. Here, the GTPase binding portion of the downstream effector is produced as a fusion protein linked to a solid-phase resin material. When the cell lysate flows through the resin, the small G proteins currently in the active form are captured, and the analysis is made by Western blotting (75-77).

2.3.3.2 Split luciferase assay

The concept of the split luciferase assay is splitting the luciferase gene into two portions so that the two protein products can only generate a chemiluminescent signal if they are in close proximity to each other, *i.e.*, fused with two interacting partners (78). If the two parts of the luciferase are bound to the small GTPase and its downstream effector protein, we can infer the amount of active small G protein from the chemiluminescent signal (79, 80) (***Figure 12***). The split luciferase system works well under *in vivo* (cell lysates, expressing exogenous and endogenous GAPs) and *in vitro* conditions (immunoprecipitated GAPs) (79).

DOI:10.14753/SE.2023.2903

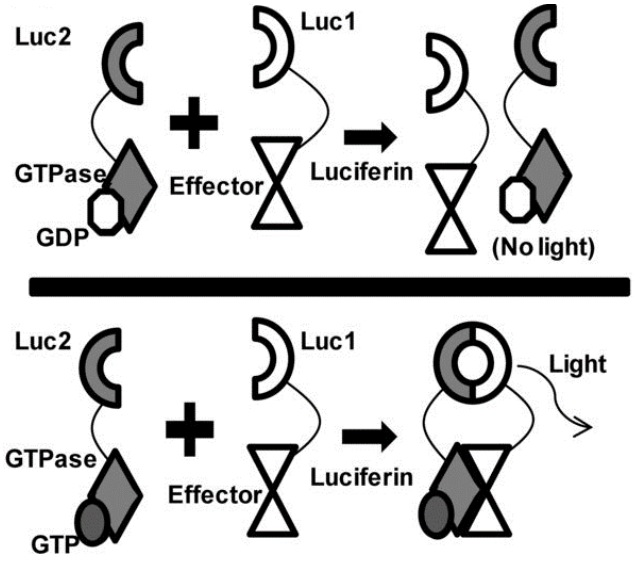

Figure 12. Schematic model illustrating the split luciferase system as a method for GTPase activity/GAP activity measurements. The two sides of luciferase are linked to the GTPase and its effector, resulting in a chemiluminescent signal only if the GTPase is in an active form (79).

2.3.3.3 FRET

Förster resonance energy transfer, or fluorescence resonance energy transfer (FRET), describes a distance-dependent, nonradiative energy transfer between two fluorophores. Upon excitation of the donor molecule, it can transfer energy to a second, longer-wavelength fluorophore (acceptor) if they are in sufficient proximity (<100 Å, ca. 1-10 nm), resulting in light emission by the acceptor (81). Therefore, the ratio between donor and acceptor emission intensities (FRET ratio) closely follows the distance between the two interacting molecules, making this technique a ’molecular ruler’ (82). Tagging molecules of interest with FRET fluorophore pairs enables studying intramolecular and intermolecular phenomena, like the interaction between small GTPases and their specific binding (effector) proteins (***Figure 13***). Furthermore, since it is a non-destructive method, it can also be used in living cells.

DOI:10.14753/SE.2023.2903

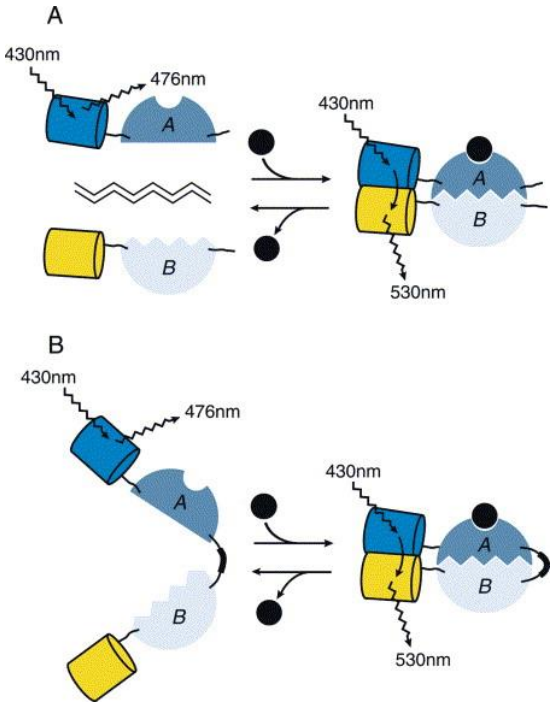

Figure 13. Schematic representation of the intermolecular (A) and intramolecular (B) fluorescence resonance energy transfer (FRET). A and B indicate the proteins/domains of interest tagged with the fluorophores (83).

2.3.3.4 Intermolecular FRET

When the small G protein and its specific binding partner are fused with the fluorophores separately, the energy transfer happens only if they are in close proximity within the cell. FLAIR (fluorescent activation indicator for Rho proteins) is a live cell imaging technique using GFP-Rac and Alexa564-PBD (p21-binding domain) as the two interacting molecules. With these, Rac localization (GFP signal) and Rac activation (FRET signal) can be followed separately, tracking the spatial distribution of Rac signaling in cellular processes (84) (***Figure 14***).

DOI:10.14753/SE.2023.2903

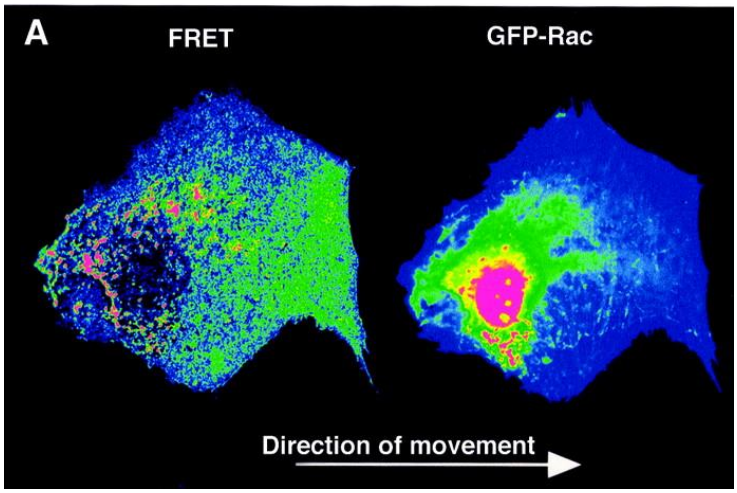

Figure 14. Rac activation (FRET) and localization (GFP-Rac) in moving Swiss 3T3 fibroblasts. Rac1 is the most active in the juxtanuclear region, and a gradient of Rac activation is also observed, which is the most prominent near the leading edge and decreasing toward the nucleus. Red represents the highest and blue the lowest intensities (84).

2.3.3.5 Intramolecular FRET

One of the first (and probably most popular) applications of FRET for observing small G protein activity was the development of the so-called Raichu (Ras and interacting protein chimeric unit) sensor (85). In this sensor, H-Ras, and the Ras-binding domain of Raf (Raf RBD) are linked to a yellow fluorescent protein (YFP) and cyan fluorescent protein (CFP) in one protein, allowing the two fluorophores to interact when active Ras binds Raf-RBD (***Figure 15***). Later, the same construct with longer linker sequences proved even more effective and resulted in a two- to three-fold larger dynamic range with lower background FRET (86).

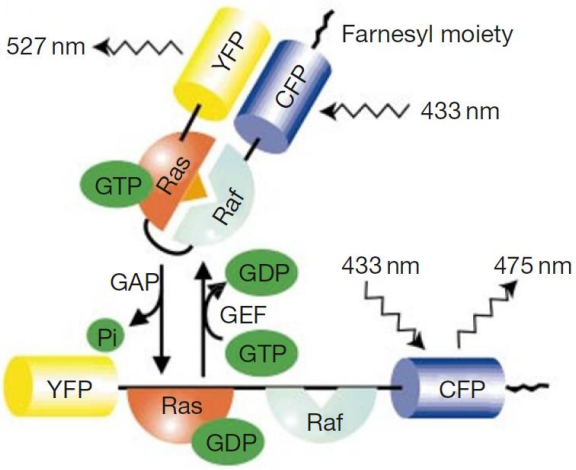

Figure 15. Design of the Raichu sensor. Energy transfer between yellow fluorescent protein (YFP) and cyan fluorescent protein (CFP) happens within the molecule when Ras is activated and binds Raf (85).

Since the small G protein-effector protein pairs can be varied, this sensor can also be utilized for monitoring the intracellular activity of other small G proteins (87).

Unfortunately, the fluorophores tend to dimerize, which can distort the binding affinities of the partners (88). One method capitalizes on this disadvantage: Graham *et al*. designed a probe where a relatively short, 44 amino acid long section of PAK is tagged with donor and acceptor fluorophores (EGFP: enhanced green fluorescent protein and EBFP: enhanced blue fluorescent protein) from both sides, generating a basal FRET signal (89). Upon binding of Rac to the EGFP-PAK-EBFP construct, energy transfer between the donor and acceptor is disrupted, and the FRET ratio decreases.

2.3.4 Comparison of the described methods

All the assays mentioned above have advantages and disadvantages, summarized in ***Table 2***. Although there is a plethora of possibilities, we still do not have a method that works for every purpose universally. Ideally, one should take into consideration the exact biological phenomenon that will be examined and the capabilities and limitations of each assay when choosing the appropriate method.

For *in vitro* analysis, both the fluorescently labeled guanine nucleotides and the high-throughput methods may be recommended. However, fluorescent mant-labeling can modify the small G protein-GAP binding properties, and it also does not work well with

all GTPase families, presumably because they differ in the conserved amino acids involved in nucleotide binding (67, 68). Moreover, removing the free mant-nucleotides (through gel filtration) is time-consuming and laborious. The easy and robust high-throughput well-based assays can facilitate the workflow, but they are relatively expensive, and since they measure an enzymatic product, they only give endpoint results. Although radiolabeling is a widely known and very reliable method, the disadvantages of this technique and the appearance of safer alternatives make it obsolete and impractical.

Affinity precipitation can be the most beneficial choice to examine the GTPase reaction in cells, preferably with endogenous proteins. However, obtaining a GAP dose-response curve is practically impossible under these circumstances, and similar to the well-based assays, it will provide endpoint results only. Also, it is one of the most labor-intensive techniques.

For live cell imaging, intramolecular FRET biosensors have been widely used due to their high signal-to-noise ratio and simple ratiometric analysis (90). However, a severe disadvantage of these sensors is that they have to be heterologously expressed in the cell, which might disrupt the quantitative distribution of endogenous proteins. Also, transiently transfecting cells with multiple vectors (*i.e.*, adding a GAP molecule) makes it difficult to reach a constant stoichiometry between experiments. Moreover, the attachment of fluorescent molecules to small GTPases may alter their interaction with upstream and downstream partners (91). Above all that, the FRET efficiency of the intramolecular FRET biosensor depends not only on the distance but also on the relative orientation of the donor and the acceptor molecules, and the latter is tough to predict (83).

I did not include the measurement of intrinsic tryptophan fluorescence in the list. Although it works reliably with many GTPases containing a highly conserved tryptophan residue – in some cases even outperforming mant-GTP labeling (92) – unfortunately, apart from Cdc42 (93), it cannot be used for other members of the Rho family, such as Rac and Rho proteins (68).

DOI:10.14753/SE.2023.2903

Table 2. Summary of the advantages and disadvantages of the GTPase activity measurements discussed in Chapter 2.3.

Method		Advantages	Disadvantages
GUANINE NUCLEOTIDE LABELING	**Filter binding assay-radiolabeling**	-reliable -sensitive	-hazardous: needs specific safety measures -expensive -produces radioactive waste -works only *in vitro* -endpoint measurement only
	fluorescent labeling of GTP and GDP	-safe -continuous monitoring	-require higher protein concentrations -works *in vitro* only
MEASUREMENT OF ENZYMATIC PRODUCTS (GTP, GDP, P_I)	**GTPase-Glo™; Transcreener® GDP Assay; EnzCheck™; CytoPhos™**	-optimal for high-throughput measurements -add-mix-read format, easy protocols	-expensive -endpoint measurement only
METHODS BASED ON SPECIFIC BINDING	**Affinity precipitation**	-works well with cell lysates -can detect endogenous small G protein	-labor-intensive -indirect analysis -no subcellular localization -endpoint measurement only
	Split luciferase assay	-works both in cell-based and *in vitro* assays -can detect endogenous small G protein	-cloning steps are needed -genetically modified small G proteins might interact with their upstream and downstream partners differently than WT counterparts
	FRET	-can detect endogenous small G protein -enables continuous live-cell imaging	-not very sensitive -prone to photobleaching -cloning steps are needed -genetically modified small G proteins might interact with their upstream and downstream partners differently than WT counterparts

DOI:10.14753/SE.2023.2903

3. OBJECTIVES

ARHGAP25's immunological importance and its newly described role in tumor cell migration and metastasis make the investigation of its regulation, primarily via phosphorylation, all the more relevant. However, our current knowledge of the exact phosphorylation sites and the effect of phosphorylation on ARHGAP25's enzymatic activity is still very limited. Therefore, during my Ph.D. studies, I aimed to:

1.) examine the phosphorylation of ARHGAP25 *in silico*, *in vitro* and *in vivo*;

2.) develop a new method that enables the measurement of *in vitro* GAP activity in a real-time manner without the need for time- and money-consuming techniques (e.g., radioactivity);

3.) investigate whether phosphorylation affects ARHGAP25's RacGAP activity *in vitro*;

4.) identify the amino acids responsible for the phosphorylation-dependent changes of ARHGAP25's GAP activity.

DOI:10.14753/SE.2023.2903

4. METHODS

4.1 Reagents

Protease Inhibitor Cocktail, Phosphatase Inhibitor Cocktail 2, Phenylmethanesulfonyl-fluoride, adenosine 5'-triphosphate, Aprotinin, Leupeptin, Pepstatin A, Diisopropyl-fluorophosphate, Dithiothreitol, Guanosine 5′-diphosphate, Guanosine 5′-[β-thio]diphosphate, Guanosine 5′-[γ-thio]triphosphate, dimethylformamide, phorbol myristate acetate, Tween-20 and pGEX-4T-1 vector were purchased from Sigma-Aldrich (St. Louis, MO, USA). One Shot™ BL21 Star™ *Escherichia coli* bacteria, Pierce™ Glutathione Agarose beads, Pro-Q™ Diamond Phosphoprotein Gel Stain, and SYPRO™ Ruby Protein Gel Stain were from Invitrogen (ThermoFisher Scientific, Waltham, MA, USA). Lambda Protein Phosphatase was obtained from New England BioLabs (Ipswich, MA, USA), GTPase-Glo™ Assay and lipofectamine-HD was from Promega (Madison, WI, USA). [γ-^{32}P]GTP was obtained from the Institute of Isotopes Co. Ltd. (Budapest, Hungary). CRIB-RLuc vector was a kind gift from Dr. András Balla, and Cerulean-C1 and mVenus-N1 vectors were a gift from Dr. Péter Várnai.

4.2 Cloning

Full-length human ARHGAP25 was cloned using cDNA from human peripheral blood cells as a template resulting in a 646 amino acids long protein. This protein corresponds to the Isoform 4 in the UniProt database (P42331-4) or the mRNA transcript variant 1 of the NCBI database (NM_001007231.2), which consists of an additional alanine at position 156 compared to the canonical sequence. It was cloned into pGEX-4T-1 and this clone was used for BRET measurements and mutagenesis. Previously, our group also worked with transcript variant 2 (NM_014882.3, coding the 638 aa-long Isoform 3 in the UniProt database) and this clone was used for generating truncated domains (PH domain, GAP domain, interdomain and coiled coil region, see ***Table 3*** for the primers and ***Figure 16*** for visual representation). Mutations were introduced via site-directed mutagenesis using the primers in ***Table 3***. Mutations were confirmed by Sanger sequencing (Microsynth AG, Balgach, Switzerland). CRIB-RLuc vector containing the extended, 83 amino acids long Cdc42/Rac interactive binding motif was amplified and cloned into pGEX-4T-1. Rac1 (wild type, Q61L and T17N) was also amplified and cloned into the mVenus-C1 backbone and then into the pGEX-4T-1 vector (***Figure 16***).

DOI:10.14753/SE.2023.2903

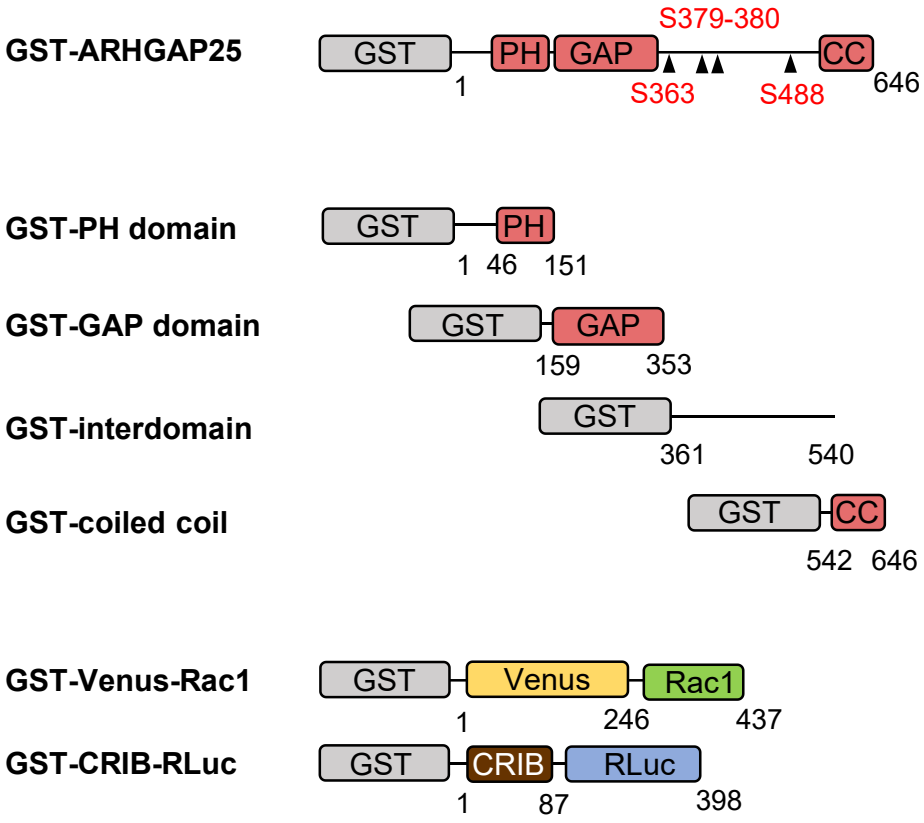

Figure 16. GST-tagged constructs used in our experiments. Full-length ARHGAP25 is a 646 amino acids long protein consisting of a pleckstrin homology (PH) domain, a GTPase activating (GAP) domain, a coiled-coil region (CC) at the C-terminus, also an 'interdomain' region between the GAP and coiled coil segments. Truncated ARHGAP25 fragments coded only the above regions. The assumed serines mutated to alanine are S363, S379-380 and S488. In the BRET-based GAP assay ARHGAP25, Venus-tagged Rac and Renilla luciferase-tagged CRIB (CRIB-RLuc) were also expressed as GST-fusion proteins.

Table 3. Primers used during cloning of ARHGAP25 constructs.

construct		Primer pairs (5' to 3' direction)
GST-PH	forward	CGGGATCCCCCATGTCCCTCGGTCAGTCGGCC
	reverse	GGAATTCGCCAAACACTCCACAGGGTGTGC
GST-GAP	forward	CGCGGATCCGCTGGCACACCCTGTGGAGTG
	reverse	GGAATTCTGACAGGGGTATATCCTTGGAC
GST-interdomain	forward	ATAGGATCCCCCCCTGCCCAGAAAAATGACC
	reverse	CCGCTCGAGTGGACTGGCAAGAGTATCTCCCTT
GST-coiled coil	forward	CGGGATCCAACTCTGAAACTGGGCCTGG
	reverse	CCGCTCGAGCCTTAAGCCTCGGTCTTGGGTTC
GST-CRIB-RLuc	forward	ATATGAATTCGGAGCAGGAATGAAAGAGAAAGAGCGGCC
	reverse	ATATCTCGAGTTACTGCTCGTTCTTCAGCACTCTC'
mVenus-Rac1	forward	ATATCTCGAGGAGCAGGACAGGCCATCAAGTGTGTGTG
	reverse	ATATGGATCCTTACAACAGCAGGCATTTTCTCTTC
S363A	forward	CCCTGGCACCCCCTGCCCAGAAAAATGACC
	reverse	CAGGGGGTGCCAGGGGTATATCCTTGGACTTGG
S379-380A	forward	CCCGAGCCGCTGT AGGCTGGGATGCCACTG
	reverse	GCCTACAGCGGCTCGGGCCACTGGAGCTTTCTTGG
S488A	forward	ACGATGGCTCAAGACTTGCGCCAACTTTCTG
	reverse	GTCTTGAGCCATCGTTCTCCTGTGCCCTTCC
R200A	forward	ATCTTCGCTCTGCCTGGGCAGGACAACCTGG
	reverse	CCCAGGCAGAGCGAAGATGCCCTCTTCATTCCGG

4.3 Preparation of primary human neutrophilic granulocytes

Venous blood was drawn from healthy adult volunteers in accordance with the Declaration of Helsinki and approved by the National Public Health Center of Hungary (31937-7/2020/EÜIG). Neutrophilic granulocytes were prepared using dextran sedimentation followed by Ficoll-Paque gradient centrifugation as previously described (94).

4.4 Protein purification

Glutathione S-transferase (GST) fusion proteins were produced in One Shot™ BL21 Star™ *Escherichia coli* bacteria. Log-phase bacterial cells expressing GST-fusion proteins were induced with 0.5 mM isopropyl 1-thio-β-d-galactopyranoside (IPTG) at 37°C for 3 hours. Bacterial pellets were lysed by sonication in a solution containing 50 mM Tris (pH 7.6), 50 mM NaCl, 5 mM $MgCl_2$, and 1 mM dithiothreitol (DTT), and before lysis, it was supplemented with 1 mM phenylmethylsulfonyl fluoride (PMSF), 1 mM Na-EGTA, 10 µg/mL aprotinin, 10 µM leupeptin and 2 µM pepstatin A. After a centrifugation step at 8,000 g for 20 minutes at 4°C, the supernatant was incubated with Pierce™ Glutathione Agarose beads for 30 minutes at 4°C and the beads were washed three times afterward with lysis buffer. Samples on beads were stored at -80°C until further use. After preparation, the protein concentration was determined according to Bradford. Additionally, protein concentrations were again checked and normalized immediately before the experiment using Nanodrop.

4.5 Phosphorylation of recombinant GST-ARHGAP25

A total of 100 µg GST-tagged recombinant ARHGAP25 protein (still on agarose beads) was incubated with 150 µL of cytosolic extract from primary human neutrophils (intact or heat-inactivated, in which case extracts were heated for 15 minutes at 100°C) in the presence of 30 µL kinase buffer (20 mM Tris-HCl, pH 7.4, 10 mM $MgCl_2$, 0.1 mM Na-EGTA, 1 mM dithiothreitol (DTT), 1% Phosphatase Inhibitor Cocktail 2, 1% Protease Inhibitor Cocktail, 1 mM PMSF and 1 mM adenosine 5'-triphosphate (ATP) for 30 minutes at 30°C.

After washing three times in washing buffer (20 mM Tris-HCl, 5 mM KCl, 1.5 mM $MgCl_2$, and 1 mM DTT), GST-ARHGAP25 was eluted from Pierce™ Glutathione Agarose beads with a buffer containing 5 mM reduced glutathione.

Dephosphorylation was carried out using 400 U Lambda Protein Phosphatase in a total volume of 50 µL for 30 minutes at 30°C before elution.

4.6 Staining of recombinant ARHGAP25 after phosphorylation

Recombinant ARHGAP25 proteins were run in SDS-PAGE gels, fixed, and stained with Pro-Q™ Diamond Phosphoprotein Gel Stain according to the manufacturer's instructions. After imaging, the same gels were stained with SYPRO™ Ruby Protein Gel Stain for the total protein amount. For imaging, we used a Typhoon 9410 (Amersham

Biosciences, Amersham, United Kingdom) with a 532 nm excitation laser and a 560 nm long-pass filter for Pro-Q™ Diamond staining and 610 band-pass filters for SYPRO™ Ruby staining.

4.7 Phosphor screen autoradiography of radiolabeled ARHGAP25

100 µg GST-tagged, recombinant full length ARHGAP25 or its truncated versions were incubated with 200 µL cytosolic extract from primary human neutrophils in the presence of 30 µL kinase buffer (20 mM Tris-HCl, pH 7.4, 10 mM $MgCl_2$, 0.1 mM Na-EGTA, 1 mM dithiothreitol (DTT), 1% Phosphatase Inhibitor Cocktail 2, 1% Protease Inhibitor Cocktail, 1 mM PMSF) completed with 10 µCi ^{32}P-ATP and 20 µM ATP for one hour at 37°C. After washing three times in washing buffer (20 mM Tris-HCl, 5 mM KCl, 1.5 mM $MgCl_2$, and 1 mM DTT), GST-ARHGAP25 was eluted from Pierce™ Glutathione Agarose beads with 2x Laemmli buffer by boiling the contents on 100ºC for 8 minutes. The supernatant was removed and run in 12% SDS-PAGE gel. After staining with Coomassie blue, we dried the gel, and the autoradiograph was taken on a phosphor screen with an exposure time of 48 hours and developed with a Bio-Rad GS-525 Molecular Imager®.

4.8 GAP activity measurements

4.8.1 In vitro Bioluminescence Resonance Energy Transfer (BRET)

Measurements were carried out in 96-well plates, in 100 µl/well total volume. Each well contained 2 µg GST-CRIB-RLuc dissolved in 20 mM Tris-HCl buffer (pH 7.5) and 5 µg GST-Venus-Rac1. The fluorescence of the latter protein was also measured before each experiment to confirm that not only the concentration, but the fluorescence intensity was identical between experiments. Before adding it to the reaction, GST-Venus-Rac1 was preincubated (’loaded’) with 30 µM GTP (or 300 µM GTPγS or GDPβS for positive and negative controls, respectively) for 10 minutes at room temperature in a low magnesium binding buffer (16 mM Tris-HCl, pH 7.5, 20 mM NaCl, 5 mM EDTA). Incubation of Rac was stopped, and GTP-binding was stabilized by adding 25 mM $MgCl_2$ so that all the Rac proteins were in an active conformation. Then, Renilla luciferase substrate coelenterazine h (5 µM) was added complemented with 1 mM GDP. Finally, the reaction was started by the addition of 15 µg GST-ARHGAP25, as indicated in ***Table 4***. The amount of GST-ARHGAP25 (µg/well) was optimized based on its dose-response curve on Rac’s GTPase

activity. Emissions were measured every 30 seconds for 15 minutes using 535-30 nm (Venus) and 475-30 nm (RLuc) filters at 25°C on a CLARIOStar luminometer (BMG Labtech, Ortenberg, Germany). Results were analyzed with MARS Data Analysis Software (BMG Labtech, Ortenberg, Germany). All BRET measurements were performed in duplicates, and BRET ratios were calculated by dividing the 535 nm and 475 nm intensities. The BRET ratio of wells containing unloaded GST-Venus-Rac1 and GST-CRIB-RLuc was used as background and subtracted from the stimulus-induced BRET ratios (***Table 4***). The BRET ratio was normalized to the 0 min value in each sample and expressed as the percentage thereof.

Table 4. Experimental design of the BRET-based GAP assay†.

Content: / Sample Name:		Rac only	ARHGAP25	ARHGAP25-P	PC	NC	background
GST-CRIB-RLuc		+	+	+	+	+	+
GST-Venus-Rac1 pretreated with:	none	-	-	-	-	-	+
	GTP	+	+	+	-	-	-
	GTPγS	-	-	-	+	-	-
	GDPβS	-	-	-	-	+	-
GST-ARHGAP25 pretreated with:	intact cytosol	-	-	+	-	-	-
	HI cytosol	-	+	-	-	-	-
coelenterazine h		+	+	+	+	+	+

†Abbreviations: PC: positive control, NC: negative control, GST: glutathione-S-transferase; CRIB: Cdc42- and Rac-interactive binding domain; GTPγS: guanosine 5'-O-[gamma-thio]triphosphate; GDPβS: guanosine 5'-O-[2-thio]diphosphate; HI: heat inactivated

4.8.2 GTPase-Glo™ Assay

The GTPase activity of different concentrations of ARHGAP25 was measured using the GAP-stimulated GTPase activity protocol of GTPase-Glo™ Assay. 2 µg GST-Rac was loaded with 1 µM GTP, and 0.5, 1, 5, or 10 µg recombinant GST-ARHGAP25 was added in a final reaction volume of 25 µl on 96-well plates. Reactions were incubated for 30 minutes at room temperature. Then, 25 µl GTPase Glo™ Reagent and 50 µl Detection Reagent were added according to the manufacturer's instructions. Luminescence (relative luminescence unit – RLU) was recorded using a CLARIOStar luminometer (BMG

Labtech, Ortenberg, Germany) and represents the amount of remaining intact GTP in the assay. RLU was normalized to a positive control (PC) and was shown as a percentage. GTP without Rac or ARHGAP25 served as a positive control, and Rac without GTP and ARHGAP25 as negative control (NC).

4.8.3 Filter binding assay with radiolabeled GTP

The GTPase activity was measured with the nitrocellulose filter-binding assay, described previously (3). GST-Rac1 was loaded with [γ-^{32}P]GTP (more than 5000 Ci/mM) for 10 min at room temperature in low magnesium binding buffer (16 mM Tris-HCl, pH 7.5, 20 mM NaCl, 0.1 mM dithiothreitol (DTT)), 5 mM EDTA, 100 nM [γ-^{32}P]GTP [5 μCi]). Then, $MgCl_2$ was added in 20 mM final concentration (for 5 min on ice) to inhibit further nucleotide exchange. The reaction was started by adding 150 ng [γ-^{32}P]GTP-loaded Rac to the assay buffer (16 mM Tris-HCl, pH 7.5, 0.1 mM DTT, 1 mg/mL bovine serum albumin, and 1 mM unlabeled GTP) containing 375 ng unphosphorylated or phosphorylated GST-tagged recombinant ARHGAP25 in a total volume of 30 μL. Next, aliquots were removed every 5 minutes, and samples were filtered through pre-wetted nitrocellulose membranes (0.45 μm pore size), followed by washing two times with 2 mL of cold buffer (50 mM Tris-HCl and 5 mM $MgCl_2$; pH 7.7). After the filters were dried, radioactivity was measured using a Beckman LS 5000TD liquid-scintillation spectrometer (Beckman Coulter, Brea, CA, USA). GAP activity was shown as the decrease in Rac-bound ^{32}P[GTP] radioactivity retained on the filters (proportional to the active Rac amount).

4.9 Statistical analysis

All data were analyzed and plotted using GraphPad Prism 8.0.1 Software. Comparison of experimental groups was carried out with paired or unpaired *t-test*, one-way ANOVA, or two-way ANOVA followed by Tukey's post hoc test, depending on the condition. All p values <0.05 were considered statistically significant.

DOI:10.14753/SE.2023.2903

5. RESULTS

5.1 Investigation of ARHGAP25's phosphorylation

5.1.1 *In silico* evaluation of potential phosphorylation sites

In order to identify possible phosphorylation sites in the ARHGAP25 sequence, we first conducted *in silico* data analysis. We searched for phosphorylation predictions in four servers: NetPhos 3.1, Group-based Prediction System 5.0, MusiteDeep, and KinasePhos 3.0. All the above use computational prediction to identify the most probably phosphorylated amino acids and, in some cases, their kinases as well. All programs found several phosphorylatable residues within the ARHGAP25 structure; 29 amino acids were present in all four predictions. ***Table 5*** summarizes the prediction analysis for full-length ARHGAP25 in the four examined databases.

Table 5. Potential phosphorylation sites found in all four in silico databases (NetPhos 3.1, Group-based Prediction System 5.0, MusiteDeep, and KinasePhos 3.0). S: serine; T: threonine.

amino acid position	phosphorylatable amino acid
2	S
25	S
40	T
222	S
336	T
363	S
379	S
380	S
392	S
396	S
399	S
402	S
404	S
408	S
443	T

amino acid position	phosphorylatable amino acid
472	S
475	S
486	T
488	S
495	S
497	S
508	S
512	S
534	S
537	S
539	T
546	S
604	S
617	S

DOI:10.14753/SE.2023.2903

5.1.2 ARHGAP25 is phosphorylated under *in vitro* conditions

To verify the above results, we decided to examine the phosphorylation of ARHGAP25 under *in vitro* conditions. Therefore, we incubated recombinant, GST-tagged ARHGAP25 with neutrophilic granulocyte cytosolic extract as a kinase source in the presence of radiolabeled ^{32}P-ATP. Since our protein was immobilized on glutathione beads at the time of the experiment, we could easily wash and remove cytosolic fragments after the incubation. Samples were then eluted and ran in SDS-PAGE, and radioactivity was measured directly in gel with phosphor screen autoradiography. We detected a clear phosphorylation signal after intact cytosol incubation, which was considerably weakened if the cytosol was heat-inactivated and completely disappeared when 'cold' (non-radioactive) ATP was in excess (***Figure 17***).

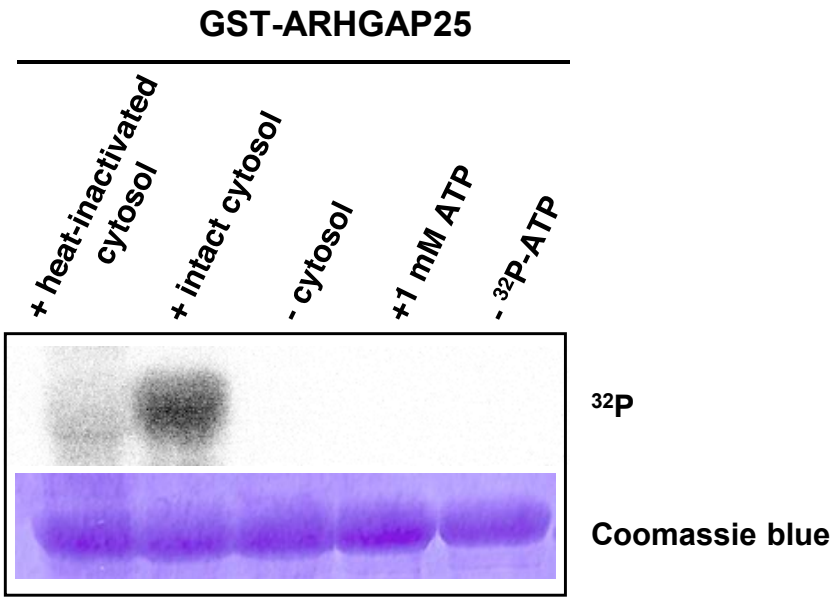

Figure 17. Incorporation of ^{32}P into ARHGAP25 in vitro. Recombinant ARHGAP25 was incubated with radiolabeled ATP and neutrophil cytosol (intact or heat-inactivated), and radioactivity was measured after 30 minutes. Coomassie blue staining (lower panel) and autoradiogram (upper panel) of the same gel are shown.

To further examine which segments of ARHGAP25 were phosphorylated, we produced truncated GST-tagged ARHGAP25 fragments containing only certain domains of the protein (GST-PH, GST-GAP, GST-interdomain, GST-coiled coil). „Interdomain" refers to a 187 AA-long region between the GAP and coiled-coil domains. As shown in ***Figure***

18, the autoradiography signal was the strongest in the interdomain region; however, the N-terminal part of the protein also displayed detectable ^{32}P-incorporation.

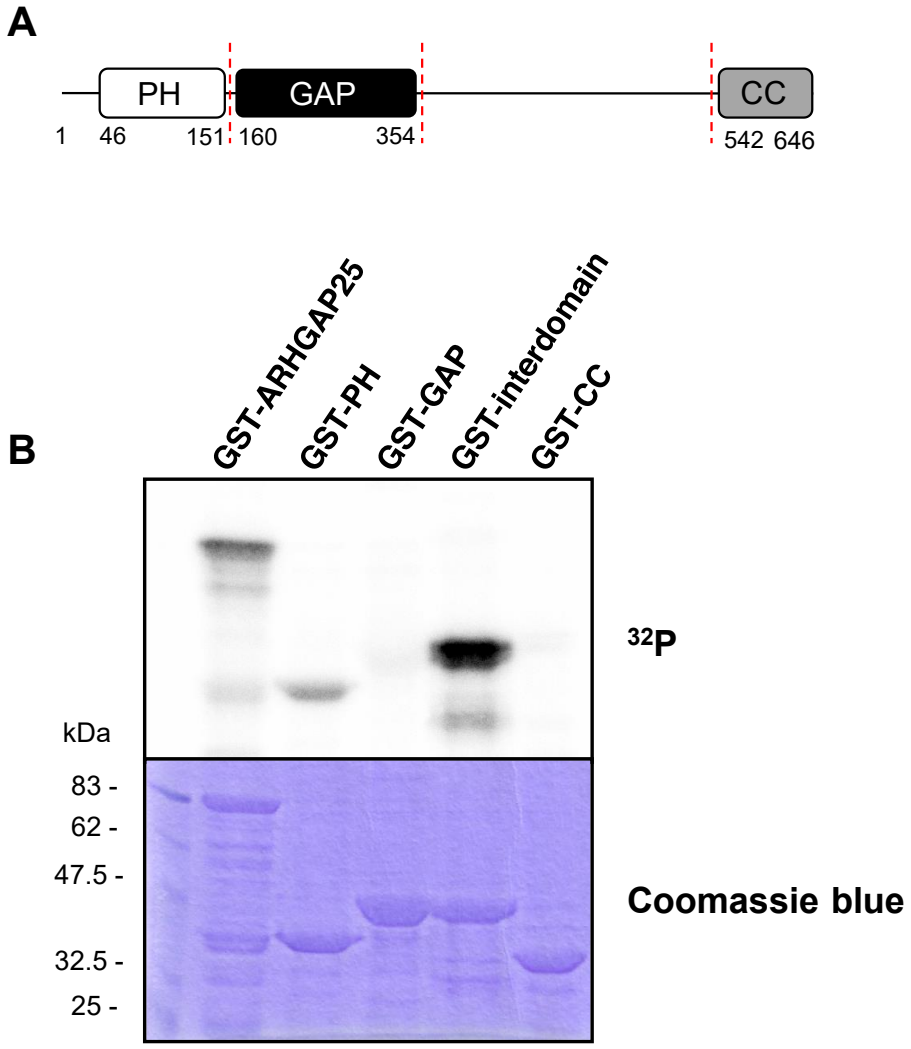

Figure 18. ^{32}P-incorporation into full-length and truncated ARHGAP25. The full-length protein was split along the red dotted lines (A). GST-tagged recombinant proteins were incubated with radiolabeled ATP and neutrophil cytosol, and radioactivity was measured after 30 minutes (B). *Coomassie blue staining (lower panel) and autoradiogram (upper panel) of the same gel are shown. Representative for two experiments.*

In order to replace the radiolabeling with a more accessible assay, we decided to assess *in vitro* ARHGAP25 phosphorylation with the Pro-Q™ Diamond Phosphoprotein Gel Stain. This assay corroborated previous autoradiography findings as intact cytosol treatment resulted in a robust phosphorylation of full-length ARHGAP25, which was not visible either with heat-inactivated cytosol or without cytosol. Lambda protein

phosphatase (LPP) treatment practically abolished the Pro-Q™ Diamond staining indicating that it, in fact, detected cytosol-induced phosphorylation (***Figure 19***).

After Pro-Q™ Diamond staining, the same gel was dyed for total protein with SYPRO™ Ruby stain, and Pro-Q™ Diamond to SYPRO™ Ruby signal ratio was regarded as phospho/total protein ratio. This was significantly higher for intact cytosol-treated ARHGAP25 compared to no cytosol or heat-inactivated cytosol treatment (***Figure 19***).

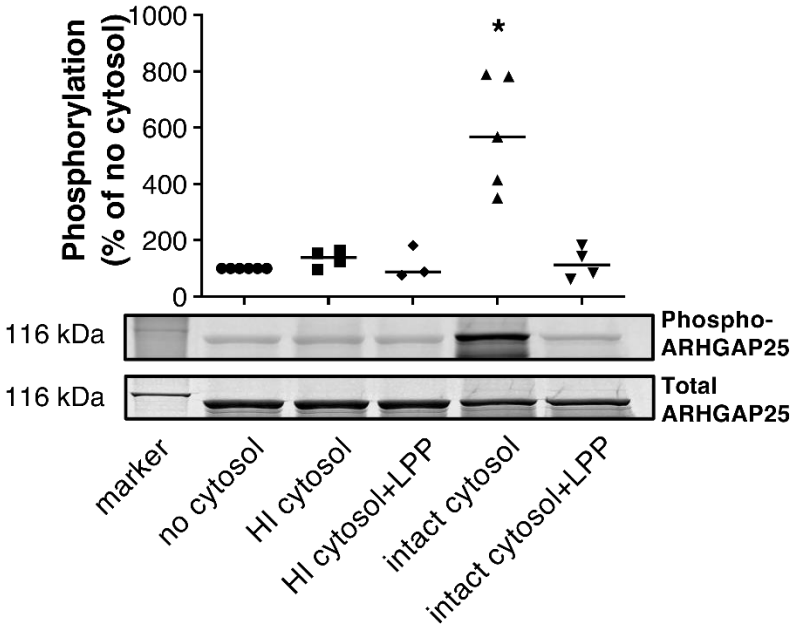

*Figure 19. Recombinant ARHGAP25 was incubated with neutrophil cytosol and stained in gel with Pro-Q™ Diamond Phosphoprotein Gel Stain for phosphoproteins and subsequently with SYPRO™ Ruby Protein Gel Stain for total protein. The phosphoprotein/total protein ratio is shown as the percentage of non-treated ARHGAP25. Treatment with intact cytosol causes robust phosphorylation compared to heat-inactivated (HI) cytosol, and it can be reversed by lambda phosphatase (LPP) treatment. n=3-6, *p<0.05 intact cytosol treatment compared to no cytosol, Kruskal-Wallis test.*

5.1.3 Identification of the phosphorylation sites

At this point, we were confident that ARHGAP25 could be phosphorylated by kinases of the neutrophil cytosol; however, to confirm the existence of phosphorylation under *in vivo* conditions and to identify the exact phosphorylation sites, we needed further experiments. In collaboration with the Biological Research Centre in Szeged, Hungary,

we conducted mass spectrometry experiments to pinpoint phosphorylated amino acid residues in ARHGAP25. We prepared four different sample types: recombinant ARHGAP25, COS-7 cells transfected with ARHGAP25, differentiated PLB-985 cells, and human neutrophilic granulocytes, the latter two expressing endogenous ARHGAP25. Human neutrophilic granulocytes were also activated with a combination of TNFα, fMLP, and PMA, the same agents that caused a strong mobility shift in SDS gel (**Figure 7**). Total protein extracts and recombinant protein samples were immunoprecipitated and digested in column with trypsin, and the recombinant protein samples were also subjected to Fe-NTA phosphopeptide enrichment by our partners. Later, our samples were analyzed by LC-MS/MS using a nanoflow RP-HPLC on-line coupled to an Orbitrap-Fusion Lumos mass spectrometer operating in positive ion mode. ***Table 6*** and ***Figure 20*** summarize our mass spectrometry findings; all raw data is openly available in figshare at: https://doi.org/10.6084/m9.figshare.19221312

Table 6. Phosphosites in ARHGAP25, detected with mass spectrometry. Altogether, 12 amino acid residues were found to be phosphorylated.

Amino acid position	GST-ARHGAP25	COS-7	PLB-985	Neutrophilic granulocyte
S2	X			
S25	X			
S363		X	X	X
S379-380	X	X		
T394-S396	X	X	X	
S437	X			
T486				X
S488	X	X		X
S495				X
S508		X		X
S512		X		
S534		X		X

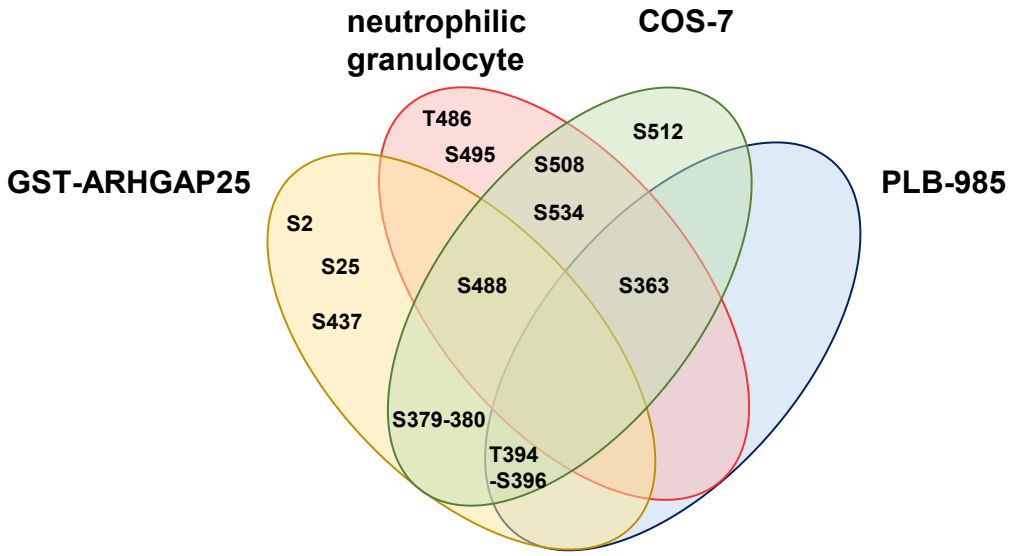

Figure 20. Venn diagram of the phosphorylated amino acids found with mass spectrometry in four different sample/cell types. S: serine; T: threonine.

We found eleven phosphorylated residues present in all datasets (MS and *in silico* analyses), most of them in the above-mentioned interdomain region (***Figure 21***). Since mass spectrometry is unable to differentiate between phosphorylation of the neighboring residues 379/380 and 394/396, we referred to them as one entity in terms of phosphorylation (S379-380 and T394-S396).

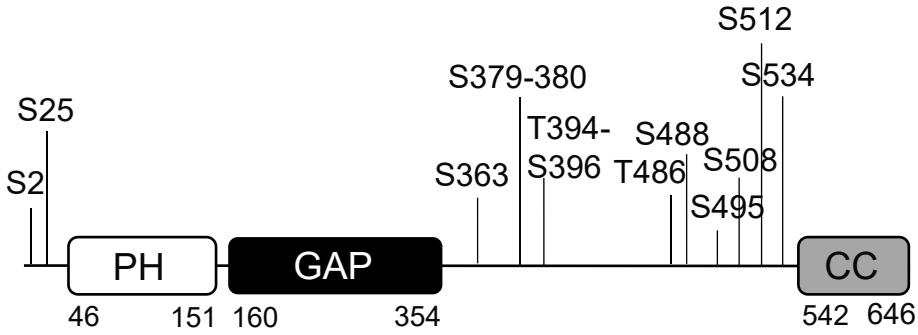

Figure 21. Based on four phosphorylation prediction sites and mass spectrometry, ARHGAP25 is phosphorylated on the indicated residues. PH: pleckstrin homology; GAP: GTPase activating protein (domain); CC: coiled coil.

5.1.4 Examining the role of S363 phosphorylation in ARHGAP25's GAP activity

In parallel experiments with our collaborators, we revealed that ARHGAP25 acts as a regulator of hematopoietic stem cell and progenitor cell (HPSC) mobilization from murine bone marrow (55). According to these results, phosphorylation on S363, S379-380, and S488 had the most significant effect on HPSC mobilization. Importantly, phosphorylation of these three residues was also consistently detected both in our *in silico* and MS experiments. Thus, we decided to focus on these three amino acids and reveal the role of their phosphorylation in ARHGAP25's function, particularly in its enzymatic (GAP) activity. To this end, we started mutating S363, S379-380, and S488 individually or in pairs to alanine (S-A mutants). The GAP activity of these mutants was then measured under control or phosphorylated (*i.e.,* treated with neutrophil cytosol) conditions and compared to that of the wild type ARHGAP25. Since ARHGAP25 phosphorylation on the S363 residue appeared to have the strongest correlation with downstream effects, that is, HPSC mobilization from bone marrow (55), we started working with the S363A mutant.

We started our measurements using the filter-binding assay with radiolabeled ^{32}P-GTP, with which our group had much experience and was readily available. In this assay, we measured the amount of active, GTP-bound Rac after adding phosphorylated or non-phosphorylated ARHGAP25. Our results showed that the *in vitro* phosphorylation of wild type ARHGAP25 by neutrophil cytosol resulted in a significant increase in active Rac amount, which refers to a decrease in its GAP activity (***Figure 22A***). However, this effect of neutrophil cytosol treatment was abolished when S363 was mutated to alanine (***Figure 22B***), strongly suggesting that phosphorylation of S363 attenuates ARHGAP25's GAP activity (***Figure 22C***).

DOI:10.14753/SE.2023.2903

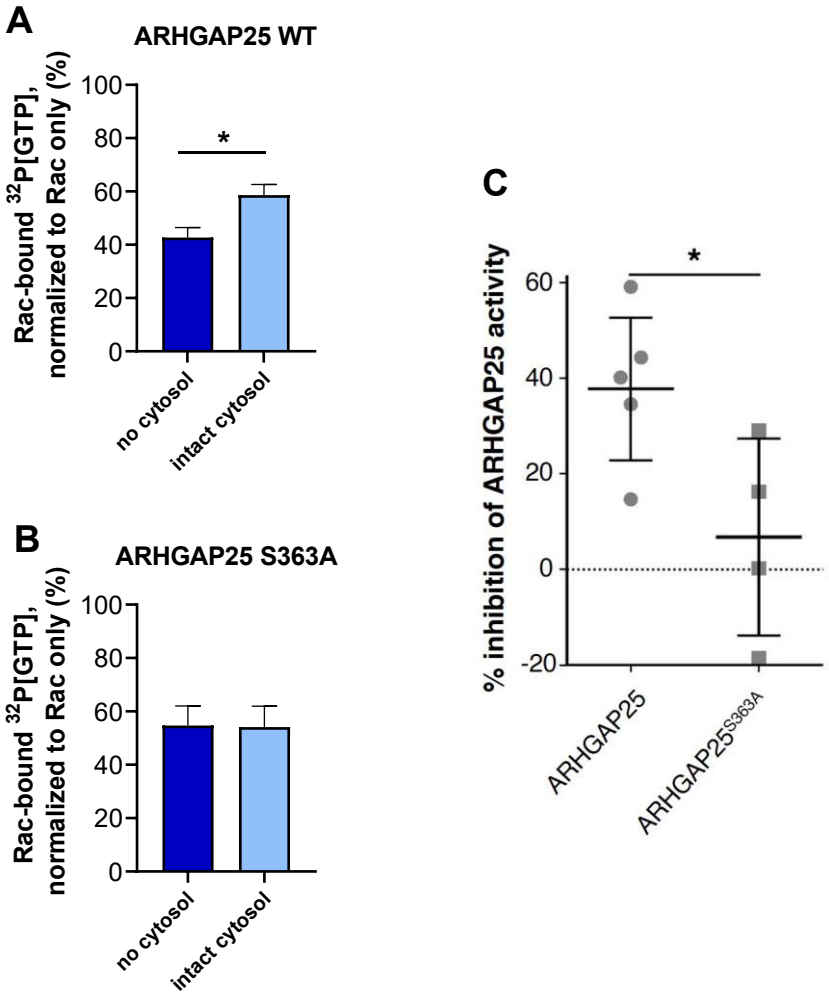

*Figure 22. Mutation of S363 affects the ability of phosphorylated ARHGAP25 to inactivate Rac. GST-tagged WT and S363A ARHGAP25 proteins were phosphorylated with intact neutrophil cytosol and ATP or were treated with ATP only (no cytosol). The GTPase effect of ARHGAP25 was measured 5 minutes after co-incubation with GST-Rac by nitrocellulose filter-binding assay. Wild type ARHGAP25 is less effective as a RacGAP after phosphorylation (A), and this difference is abolished when S363 is mutated to alanine (B). The GAP activity inhibition via phosphorylation is significantly higher in ARHGAP25 WT compared to ARHGAP25^{S363A} (C). Mean+SEM of 10 (ARHGAP25) or 4 (ARHGAP25^{S363A}) independent experiments is plotted. *p<0.05 no cytosol vs. intact cytosol treatment, two-way ANOVA and Sidak's multiple comparisons tests.*

Nonetheless, due to the many disadvantages of the radioisotope assay (see ***Table 2***), we decided to develop a new method for measuring the GAP-stimulated GTPase activity that would be more appropriate for our purposes.

5.2 Development of a bioluminescence resonance energy transfer (BRET)-based GTPase assay

5.2.1 Design and principle of our method

To investigate the role of phosphorylation in regulating ARHGAP25's RacGAP activity, we sought an alternative over the previously used radioisotope GAP assay. In addition, we wanted to start our experiments under *in vitro* conditions because the phosphorylation of ARHGAP25 can be carried out more reliably in a cell-free environment, where the exact amount of ATP and kinases can be controlled. However, currently available methods to monitor GAP activity *in vitro* seemed unsuitable for us because they either provided end-point read-outs only or were highly labor-intensive and expensive (e.g., GTPase-Glo™ Assay, filter-binding GTPase assay). These limitations prompted us to develop a new, *in vitro* bioluminescence-resonance energy transfer (BRET)-based method. To this end, we used the basic principle of intermolecular energy transfer: Rac was fused with the fluorophore Venus fluorescent protein, and the Cdc42- and Rac-interacting binding (CRIB) domain of PAK was linked to the bioluminescent *Renilla* luciferase (RLuc) (***Figure 23***). *Renilla* luciferase not only has a favorable emission spectrum for BRET, but the emission is ATP-independent, and therefore it does not interfere with other biochemical processes where ATP is involved, such as phosphorylation (95).

CRIB binds Rac only in its GTP-bound, active conformation, resulting in the molecular proximity of Venus and RLuc. In the presence of its substrate coelenterazine, RLuc excites Venus by energy transfer, causing an increase in the so-called BRET ratio, which is the emission of Venus (530 nm) divided by the emission of RLuc (480 nm). After the hydrolyzation of GTP, Rac turns to an inactive, GDP-bound form and releases CRIB, terminating the energy transfer between RLuc and Venus and thereby decreasing the BRET ratio. Therefore, the BRET ratio is proportional to the amount of active Rac. Supplementing the reaction mixture with recombinant ARHGAP25, a RacGAP should, in principle, decrease the BRET ratio (***Figure 23***).

DOI:10.14753/SE.2023.2903

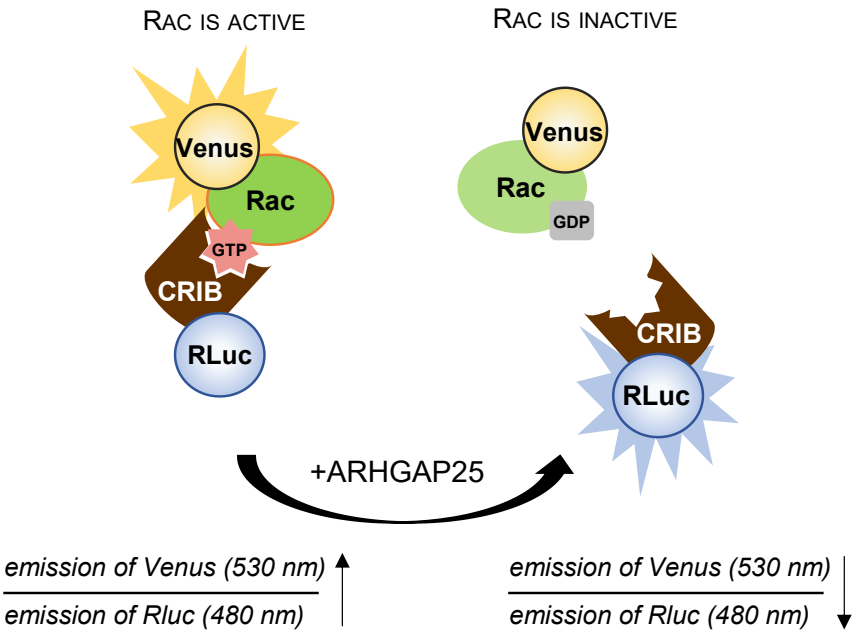

Figure 23. Schematic representation of our BRET-based GAP assay. When adding ARHGAP25 to the reaction, GTP-hydrolysis of Rac is catalyzed, and Venus-Rac detaches from CRIB-RLuc, decreasing the BRET ratio. GST: glutathione-S-transferase; CRIB: Cdc42- and Rac-interactive binding domain of PAK; RLuc: Renilla luciferase.

Since our goal was to measure the enhancement of Rac's endogenous GTPase activity by ARHGAP25, Rac needed to be in a GTP-bound, active conformation when the reaction started. Therefore, Rac was preincubated ('loaded') with GTP, and the binding was stabilized with the addition of $MgCl_2$; only after this 'loading' was Rac added to the reaction. Furthermore, to prevent Rac from binding another GTP after hydrolysis and returning to the cycle (thereby increasing the BRET ratio), we planned and performed the assay with a relatively high GDP concentration (1 mM). Under these circumstances, Rac stays in an inactive conformation after GTP hydrolysis (single turnover reaction).

5.2.2 Optimization of the quantity and ratio between the interacting partners

Finding the proper working concentrations for Venus-Rac, CRIB-RLuc, and ARHGAP25 was pivotal during assay development. We aimed to reach the optimal dynamic range for all proteins without compromising the high-throughput nature of the assay (*i.e.*, using only the minimally sufficient amounts of proteins).

DOI:10.14753/SE.2023.2903

First, we ran a luminescence assay with CRIB-RLuc only, using a series of dilutions between 1-10000-fold. As expected, the luminescence at 480 nm declined proportionally with decreasing protein amounts (***Figure 24***). To obtain a luminescence signal that is high enough at the beginning of our reaction but not too high so that we can see even minor differences, we chose the 100-fold dilution, which had an RLU of around 1 million. This corresponded to 2 μg GST-CRIB-RLuc/well.

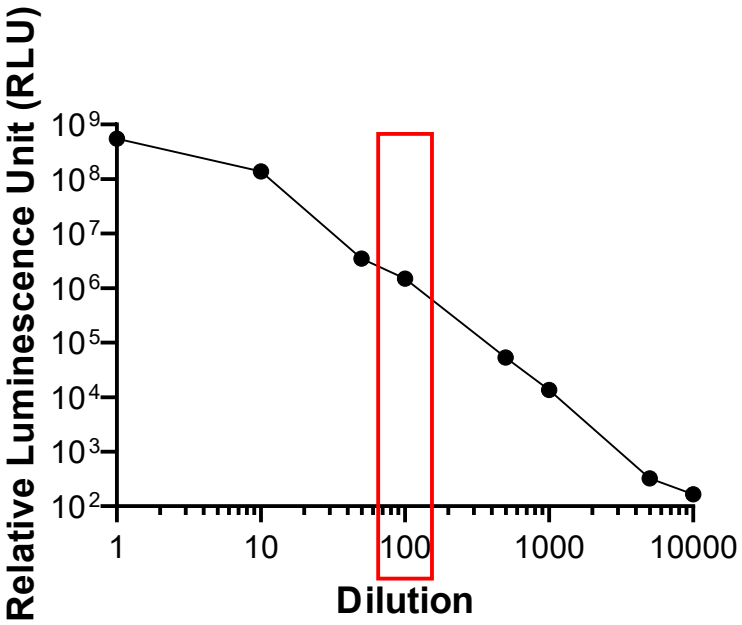

Figure 24. Luminescence of different GST-CRIB-RLuc dilutions after adding coelenterazine to the reaction (0. min). Representative data for two parallel samples.

To determine the optimal Venus-Rac amount, first we confirmed that linking Venus to Rac does not interfere with its enzymatic GTPase activity. Therefore, we measured the endogenous GTPase activity of Venus-Rac along with the untagged protein using the already established radioactive GAP assay. We observed no significant difference between Rac and Venus-Rac (***Figure 25***).

DOI:10.14753/SE.2023.2903

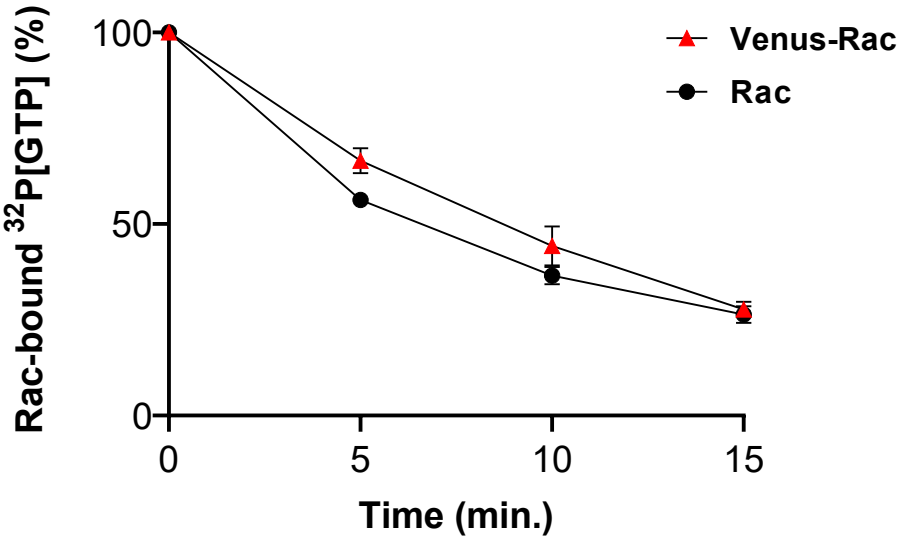

Figure 25. The fluorescent tag on Rac does not inhibit its enzymatic function. Rac's endogenous GTPase activity is seen as a decrease in radioactively labeled ^{32}P-GTP-Rac 5, 10, and 15 minutes after starting the reaction. n=5, mean ±SEM is plotted.

Next, we sought to determine the maximal and minimal achievable BRET ratios between CRIB-RLuc and Venus-Rac, in order to calculate the optimal Venus-Rac concentration. To this end, we used the previously described constitutively active (Q61L) or inactive (T17N) Rac mutants (96, 97), which can mimic a constant GTP- or GDP-bound state. Again, we used 1-10000-fold dilutions from the Rac variants with the already established CRIB-RLuc concentration. As expected, the BRET ratio in the presence of the inactive T17N Rac mutant was insensitive to Rac concentration and constituted the background signal (***Figure 26***). The constitutively active Q61L mutant showed a gradually decreasing BRET ratio with decreasing protein amounts (***Figure 26***). Based on the dilution curve, we decided to use the undiluted protein corresponding to 5 µg GST-Venus-Rac/well.

DOI:10.14753/SE.2023.2903

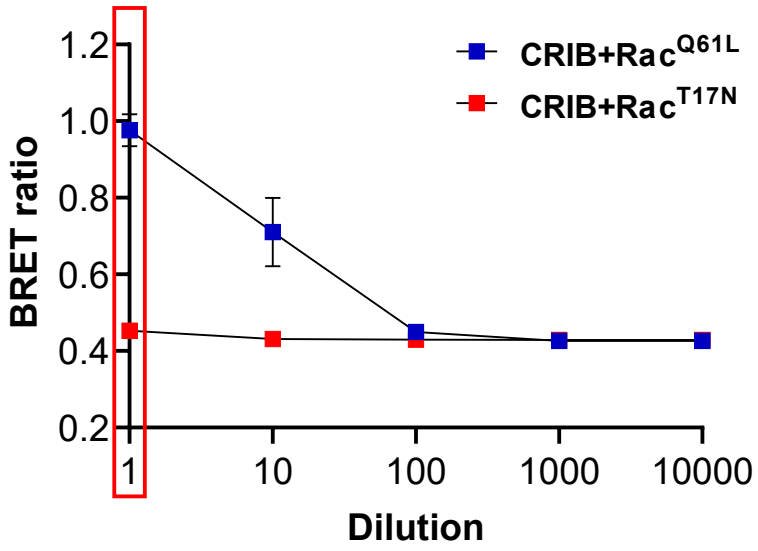

Figure 26. A constitutively active (Q61L) Venus-Rac mutant shows a relatively high BRET ratio when incubated with CRIB-RLuc. Serial dilution causes a decrease in the BRET ratio, and at a 100-fold dilution, it reaches the background level corresponding to the constitutively inactive (T17N) Venus-Rac mutant (BRET ratio was measured at 0. min after adding coelenterazine). n=4, mean±SEM is plotted.

In principle, the BRET ratio obtained with fully GTP-loaded wild type Rac at the beginning of the reaction should be very close to that acquired with the constitutively active mutant. Indeed, our observations with wild type Rac confirmed this notion (***Figure 27)***. In the previously chosen concentration (undiluted protein, 5 µg GST-Venus-Rac/well), wild type Rac's BRET ratio was between the constitutively active and inactive mutants, almost reaching the Q61L mutant's BRET ratio (***Figure 27***).

DOI:10.14753/SE.2023.2903

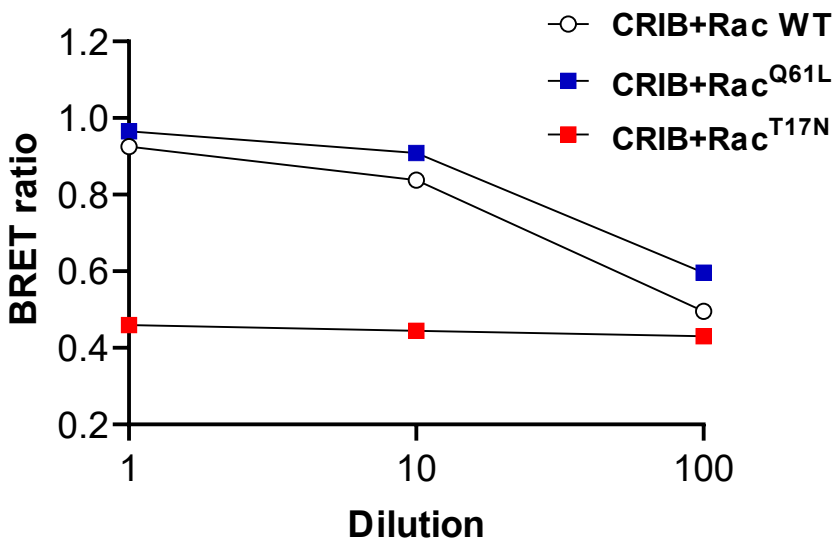

Figure 27. Decreasing concentrations of wild type, constitutively active (Q61L), and inactive (T17N) Rac were incubated with CRIB-RLuc. Wild type Rac was preloaded with GTP; therefore, its BRET ratio is very close to the Q61L mutant. The BRET ratio was measured immediately after adding coelenterazine. Representative data for 1 experiment with 2 replicates.

Next, we established the optimal ARHGAP25 concentration – one that significantly increases Rac's endogenous, slow GTP hydrolyzing activity but does not cause an immediate and drastic drop in the CRIB-RLuc – Venus-Rac BRET ratio. Therefore, we titrated the effect of ARHGAP25 between 1 to 160 µg (1, 5, 10, 20, 40, 80, and 160 µg) per well, corresponding to 0.1 and 16 µM GST-ARHGAP25. The rate of decrease in the BRET ratio was proportional to ARHGAP25 concentrations demonstrating the RacGAP activity of this protein as well as verifying the basic concept of our assay (***Figure 28A***). Considering an IC_{50} of 8.105 µg/well or 0.81 µM (***Figure 28B***), we chose 15 µg/well ARHGAP25 for subsequent experiments.

DOI:10.14753/SE.2023.2903

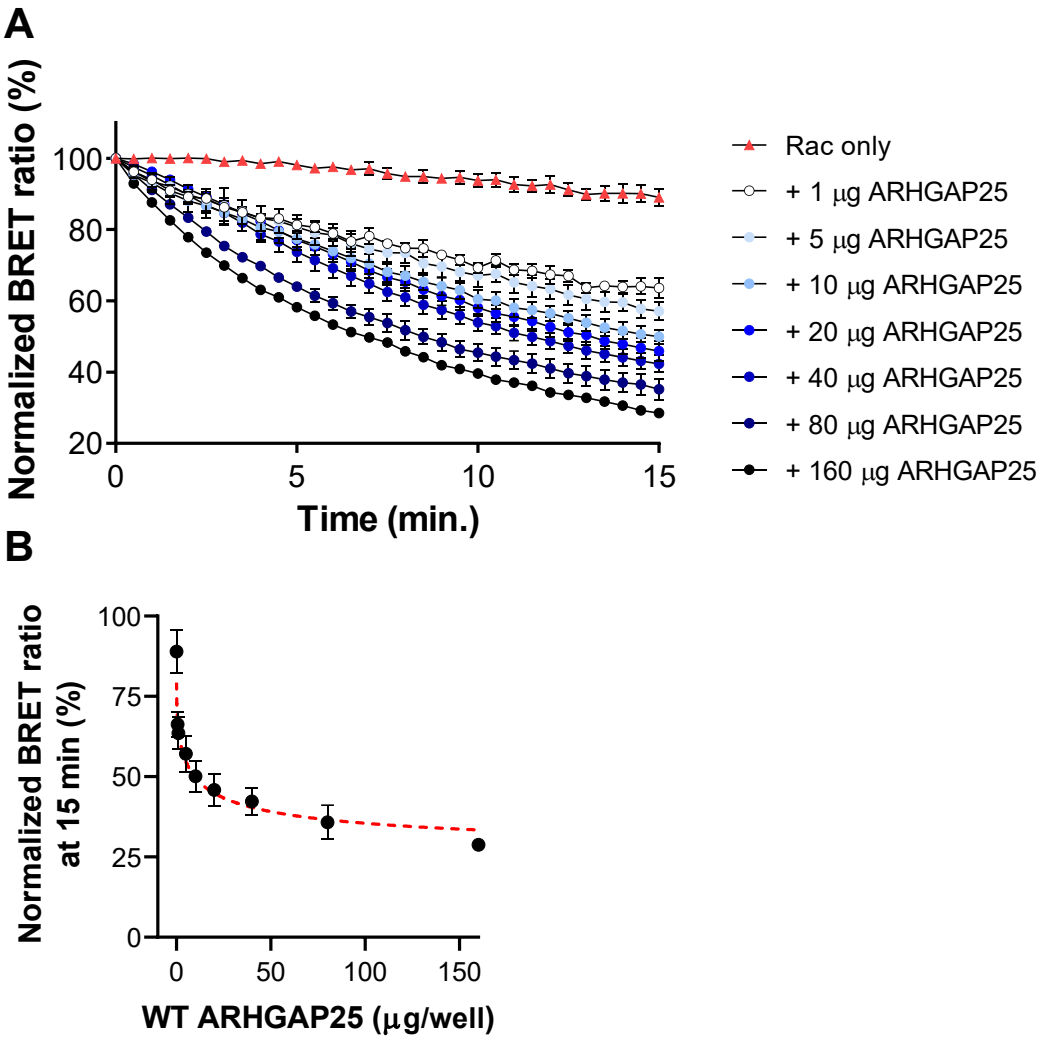

Figure 28. Dose-response curve of WT ARHGAP25 protein's effect on the GTPase activity of Rac. The amount of active, GTP-bound Rac (proportional to BRET ratio) decreases when ARHGAP25 is added to the reaction in increasing concentrations (A). For IC_{50} calculation, data points in the 15th minute of the BRET assay are plotted (B). Mean±SEM is shown, n=3 (1, 20, 40, 80,160 μg); n=5 (5 μg); n=6 (10 μg), n=7 (Rac only). R^2=0.9502.

5.2.3 Choosing negative and positive controls and measuring background activity

In order to find the best positive and negative controls for the assay and to establish the lowest and highest obtainable BRET ratios, *i.e.*, the dynamic range of the assay, we took advantage of the constitutively active and inactive mutants of Rac (Q61L and T17N, respectively) mentioned earlier. (These were loaded with the same amount of GTP as the

wild type protein.) As seen earlier (***Figures 26 and 27***), the Q61L constitutively active mutant showed a considerably higher BRET ratio than the T17N inactive mutant. The latter has an identical BRET ratio to the sample without any Rac protein (CRIB-RLuc only, no energy transfer), which further indicates that it is indeed the lowest possible BRET ratio under these circumstances (***Figure 29***).

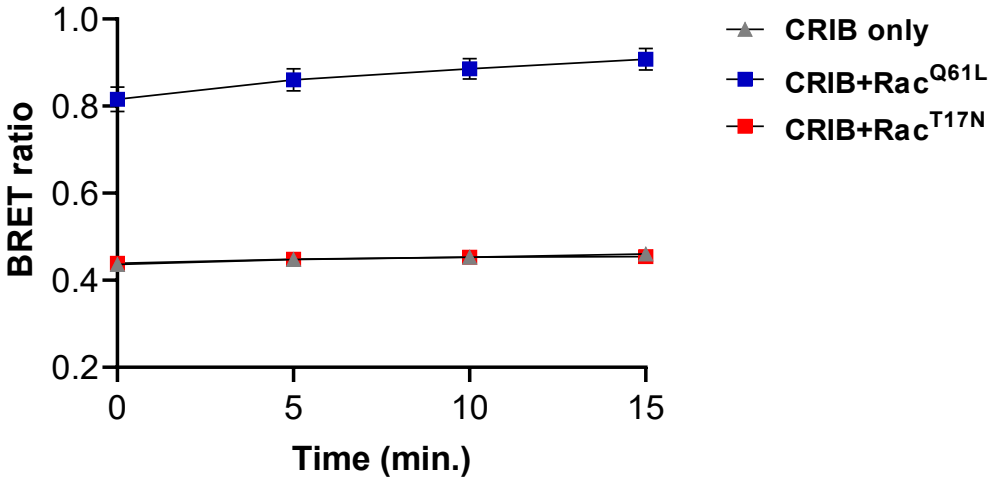

Figure 29. BRET ratios of the constitutively active (Q61L) and inactive (T17N) Venus-Rac show the lowest and highest possible BRET values during a 15-minute-long measurement. CRIB-RLuc without Venus-Rac (CRIB only) also indicates the lowest values for not being able to excite Venus, showing minimal emission at 530 nm. Mean±SEM of 3 independent experiments is plotted.

Most probably due to inherent variation in the amount of enzymatically active protein in different protein preparations (WT, Q61L, T17N), we observed some discrepancy in the initial BRET values between experimental runs. To mitigate this uncertainty, in later experiments we decided to use wild-type Venus-Rac pre-loaded with GDPβS and GTPγS, the non-hydrolyzable GDP and GTP analogs as negative and positive controls. In this setup, we could use the same amount of wild type Rac preincubated with different nucleotides, thereby decreasing the variability of BRET ratios. As a result, Venus-Rac loaded with GDPβS had a low BRET ratio very close to the samples with CRIB-RLuc only, while GTPγS-loaded Venus-Rac displayed, as expected, the highest BRET ratio of all the samples (***Figure 30A)***.

DOI:10.14753/SE.2023.2903

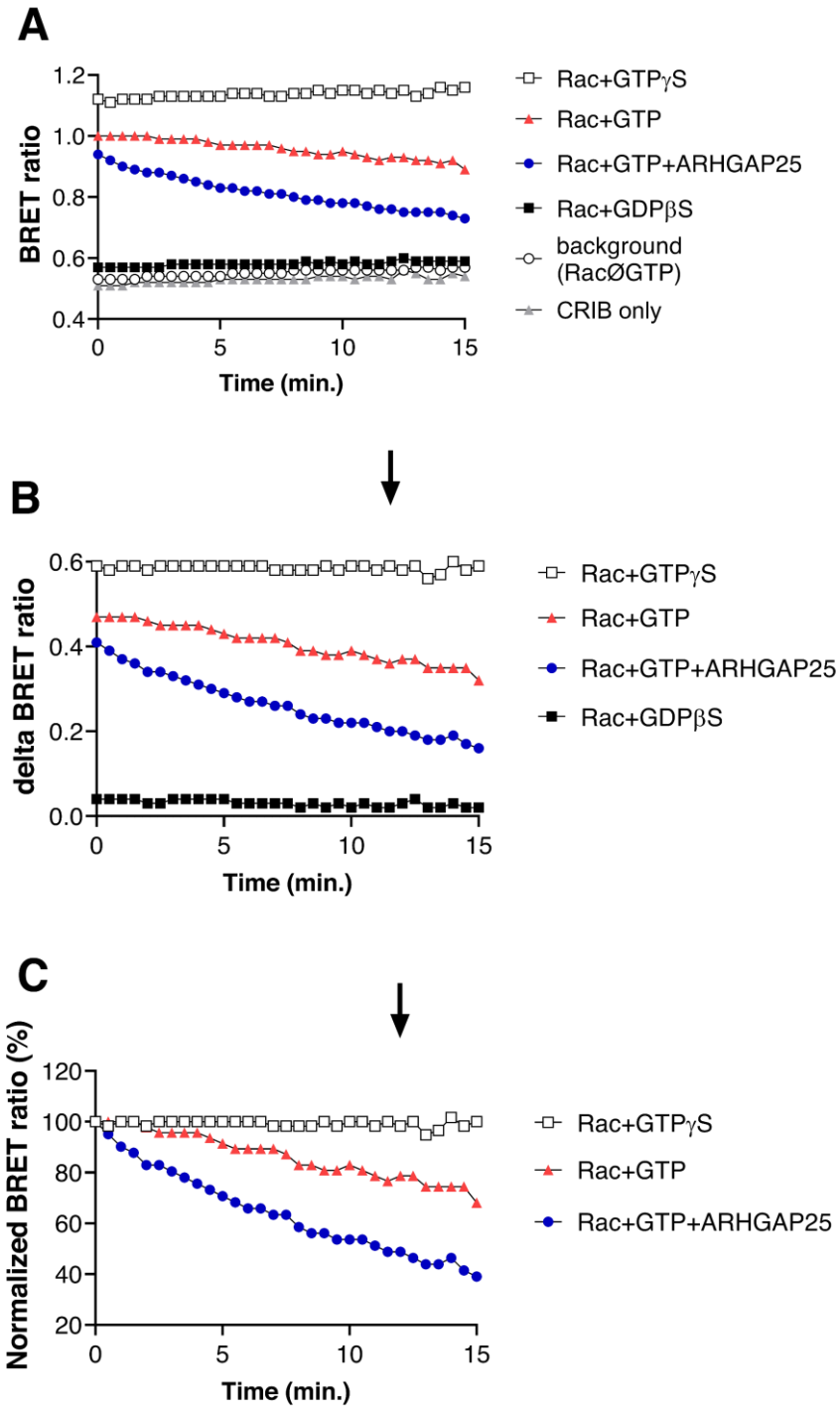

Figure 30. Process of data evaluation and presentation. Wild type Rac loaded with the non-hydrolyzable GTP analog GTPγS shows the highest BRET ratio, while samples containing CRIB only, unloaded Rac (background) or GDPβS-loaded Rac show the minimal BRET ratio (A). The background was then subtracted from the initial BRET ratios, resulting in the so-called delta BRET ratio (B). From these data points, we

calculated the percentage of the initial (0. min) BRET ratio (C). Data are representative of one experimental run with two replicates.

Notably, we observed a slight increase in the BRET ratio if Rac was loaded with GDPβS or GTPγS, a phenomenon we previously noticed with mutant Venus-Rac proteins as well (***Figure 29***). This effect was most probably caused by the gradually weakening activity of coelenterazine and the gradually decreasing emission at 480 nm and explains why the samples with CRIB-RLuc alone had the same tendency (***Figures 29 and 30A***). To offset this effect, we included samples with unloaded Rac (*i.e.*, without GTP, GTPγS, or GDPβS) and subtracted this signal (background) from all other values (delta BRET ratio, ***Figure 30B***). Finally, we normalized the BRET ratio to the initial (0. min) value (normalized BRET ratio, ***Figure 30C***); and we used this normalized BRET ratio for statistical analysis in subsequent experiments.

5.2.4 Optimization of the GTP concentration

Since our assay was derived from the previously used radioisotope assay, we decided to work with the already established 30 μM GTP for Rac loading (27). Keeping the GTP concentration relatively low (intracellular concentration is around 0.5 mM (98)) was important to prevent the repeated GTP-binding of Rac. Nonetheless, we also carried out the BRET assay with Venus-Rac loaded with 0.1 mM, 1 mM, or 10 mM GTP and revealed that different GTP concentrations did not drastically affect the assay characteristics. (It has to be noted that the raw BRET ratio started at a significantly lower level with 10 mM GTP compared to smaller concentrations (data not shown)). More importantly, the addition of ARHGAP25 significantly accelerated Rac inactivation regardless of the GTP concentration (***Figure 31***). All things considered, we opted for the original 30 μM GTP concentration to ensure the single-cycle approach.

DOI:10.14753/SE.2023.2903

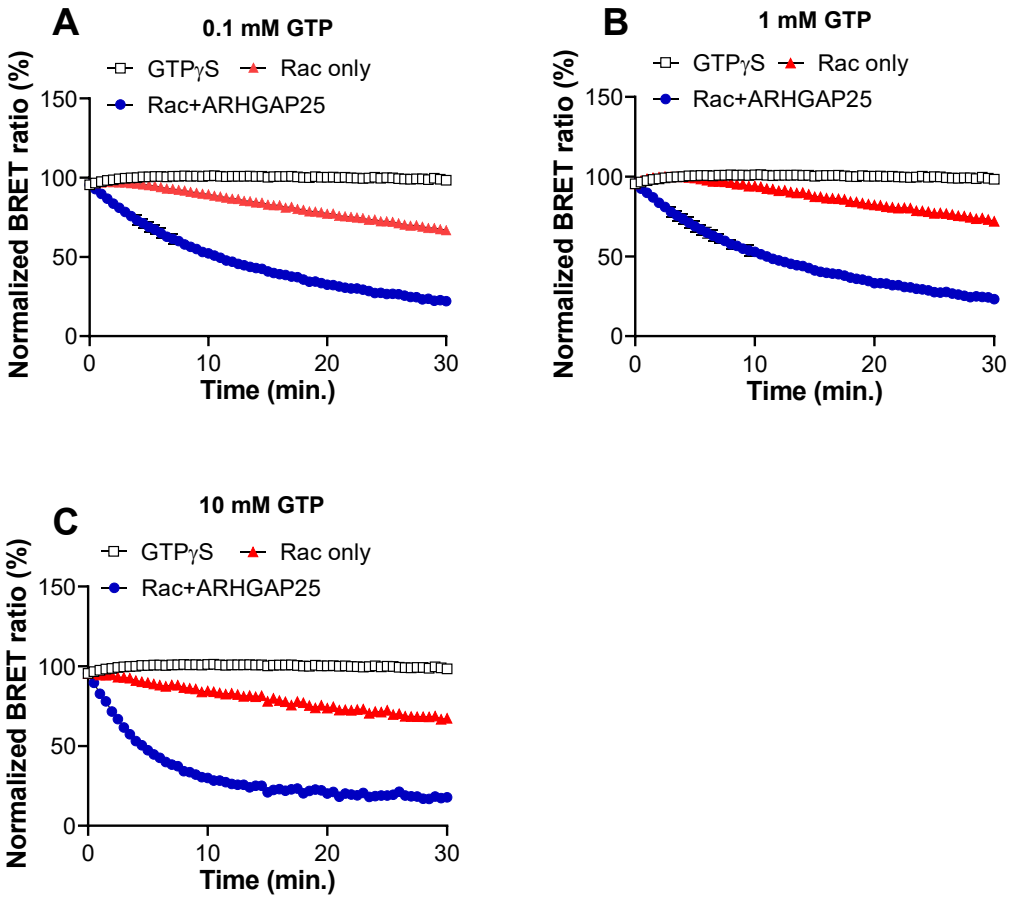

Figure 31. Normalized BRET ratio of Rac ± ARHGAP25. Rac was loaded before the experiment with 0.1 mM (A), 1 mM (B), or 10 mM GTP (C). The mean is plotted. n=2 with two replicates/run (GTPγS, 0.1 mM and 1 mM GTP); n=1 with two replicates/run (10 mM GTP).

The final concentrations of the optimized assay are displayed in ***Figure 32.*** and ***Table 7.***

DOI:10.14753/SE.2023.2903

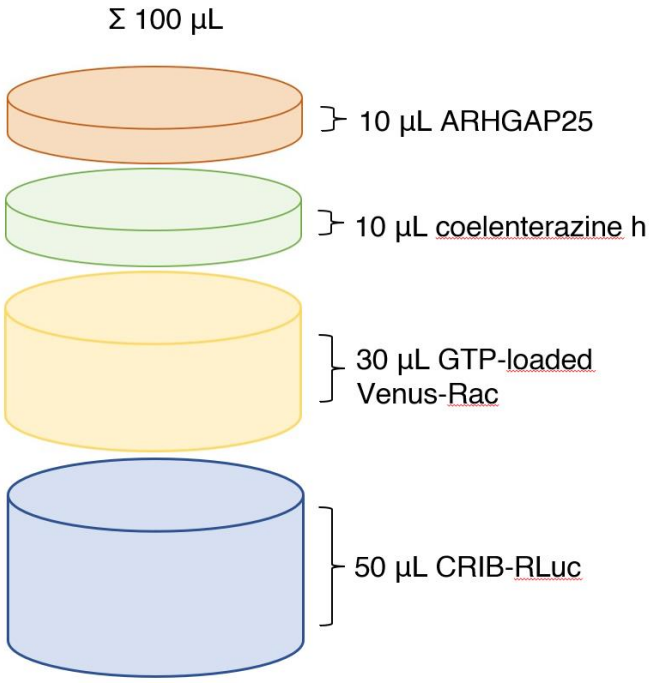

Figure 32. Composition of a well in a 96-well plate during the BRET-based GAP assay. The final reaction volume is 100 µl.

Table 7. Final concentrations of the components in the BRET-based GAP assay.

Volume	Content	Final concentration (in 100 µL)	Notes
10 µL	GST-ARHGAP25	150 ng/µL (1.5 µM)	added directly before the measurement
10 µL	coelenterazine h	5 µM	
	GDP	1 mM	added only after GTP loading
30 µL	GST-Venus-Rac	50 ng/µL (660 nM)	dissolved in a low magnesium binding buffer (pH 7.5)
	GTP	10 µM	concentration during Rac loading: 33 µM
	GTPγS/GDPβS	0.1 mM	concentration during Rac loading: 0.3 µM
	Na-EDTA	1.5 mM	concentration during Rac loading: 5 mM
	$MgCl_2$	7.5 mM	added only after GTP loading, the concentration is 25 mM during GTP stabilization
50 µL	GST-CRIB-Rluc	20 ng/µL (435 nM)	dissolved in 20 mM Tris-HCl buffer (pH 7.5)

5.2.5 Assay validation

After optimizing the BRET reaction, we compared this new BRET GAP assay with the previously used radioisotope filter-binding approach. Both assays detected the endogenous GTP-hydrolysis of Rac as a slight decrease in active Rac amount, however, the BRET assay allowed substantially better temporal resolution (***Figure 33***) while being less labor intensive. Again, the addition of wild type recombinant ARHGAP25 accelerated the endogenous GTP hydrolysis of Rac (***Figure 33***).

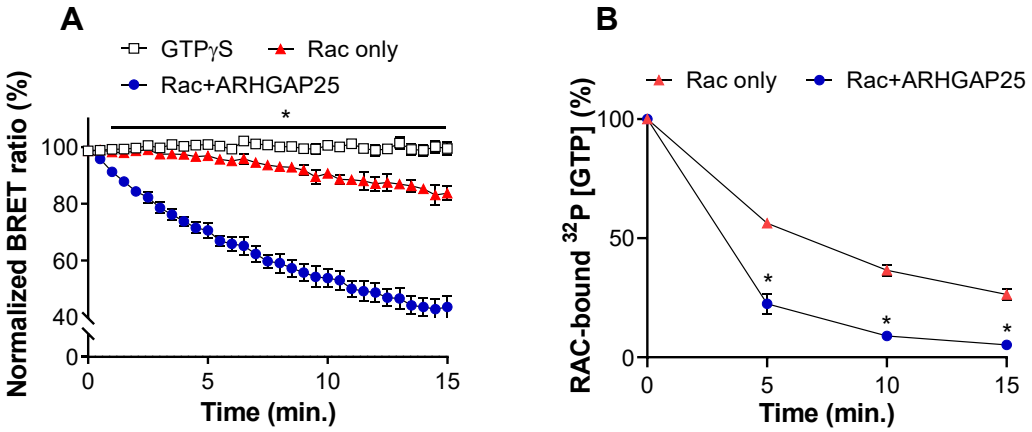

*Figure 33. Wild type ARHGAP25 enhances Rac's weak endogenous GTPase activity. Mean±SEM of 4 independent experiments is plotted. Significance is shown in a from-to interval, *p<0.05 ARHGAP25 compared to Rac, two-way ANOVA with Tukey post-hoc test (A). Radioisotope GAP assay shows ARHGAP25's GAP activity as a decrease in isotope-labeled Rac-GTP. Mean±SEM of 5 independent experiments is plotted, *p<0.05 Rac+ARHGAP25 compared to Rac, two-way ANOVA (B).*

Although we have already established that our assay can distinguish between small differences in ARHGAP25 concentrations (***Figure 28A)***, we also wished to compare its sensitivity to two widely used GTPase assays, the radioisotope and the commercially available GTPase-Glo™ approaches. As shown in ***Figure 34***, BRET results were not only comparable to those obtained with the established procedures but provided higher sensitivity and generally less variance, not to mention the best temporal resolution. Taken together, we showed that our novel approach is appropriate for monitoring ARHGAP25's GAP activity in real time with high fidelity.

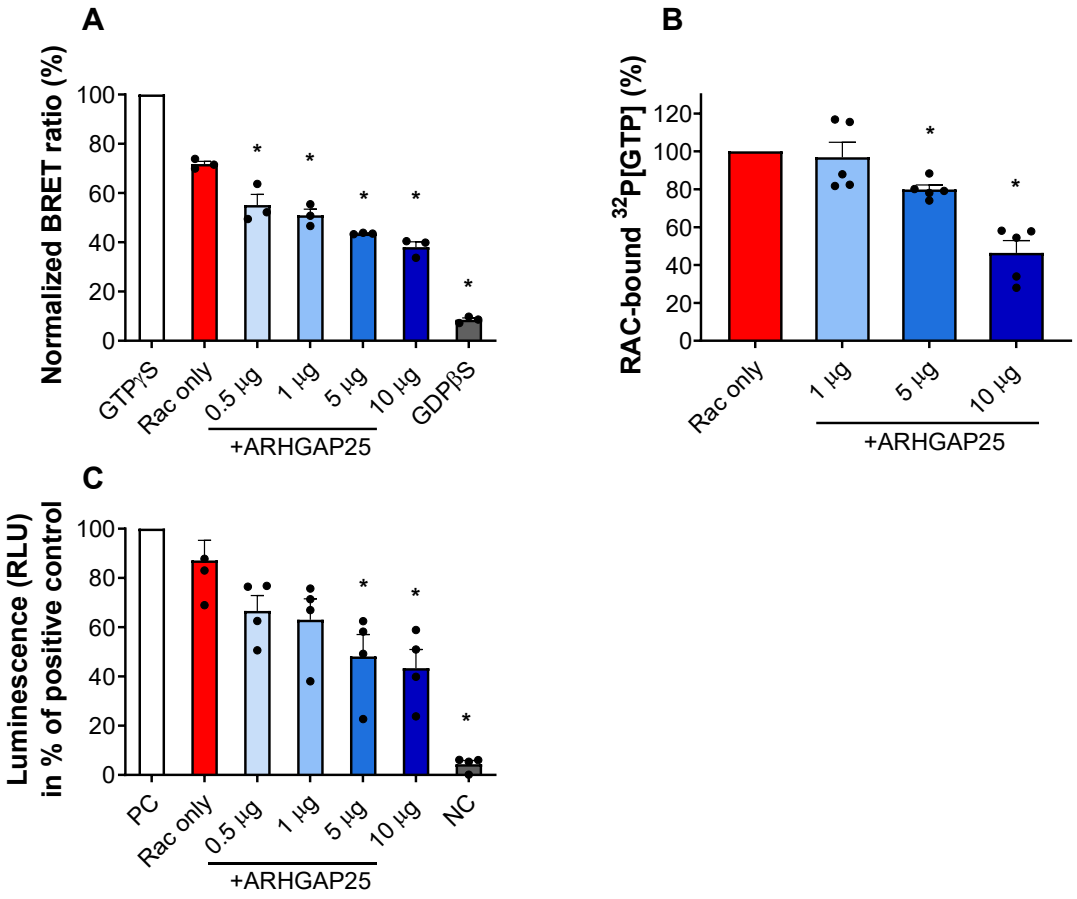

*Figure 34. BRET-based GAP assay (A); radioisotope filter-binding GAP assay (B); and Promega's GTPase-Glo™ Assay (C) show the dose-dependency of ARHGAP25's GTPase activating effect 15 minutes after the indicated amount of ARHGAP25 was added to Rac. The mean+SEM of three (A, C) and five (B) independent experiments is plotted. *p<0.05 '+ARHGAP25' compared to Rac using one-way ANOVA analysis. PC: positive control, NC: negative control.*

Taken together, we showed that this novel approach is reliable for real-time monitoring of ARHGAP25's GAP activity.

5.2.6 Measuring the effect of phosphorylation on ARHGAP25's GAP activity

Taking advantage of our new method of measuring RacGAP activity, we started to investigate how phosphorylation affects ARHGAP25's GAP activity. The

phosphorylation protocol was similar to what we used when staining phosphoproteins in SDS gel. Namely, we incubated recombinant GST-tagged ARHGAP25 with neutrophil cytosol extract and 1 mM ATP for 30 minutes. Non-phosphorylated wild type ARHGAP25 significantly reduced the active Rac amount by its relatively high GAP activity. In contrast, phosphorylated ARHGAP25 was less active as a GAP (***Figure 35)***. As negative controls, heat-inactivated (HI) cytosol and buffer without any cytosol were used. Buffer-only (no cytosol) samples did not differ from the HI cytosol-treated ones (***Figure 35***), nevertheless, the latter contains all cytosolic proteins and fragments with inactive enzymes. Therefore, we chose the HI cytosol treatment as a control containing non-phosphorylated ARHGAP25 in the following experiments.

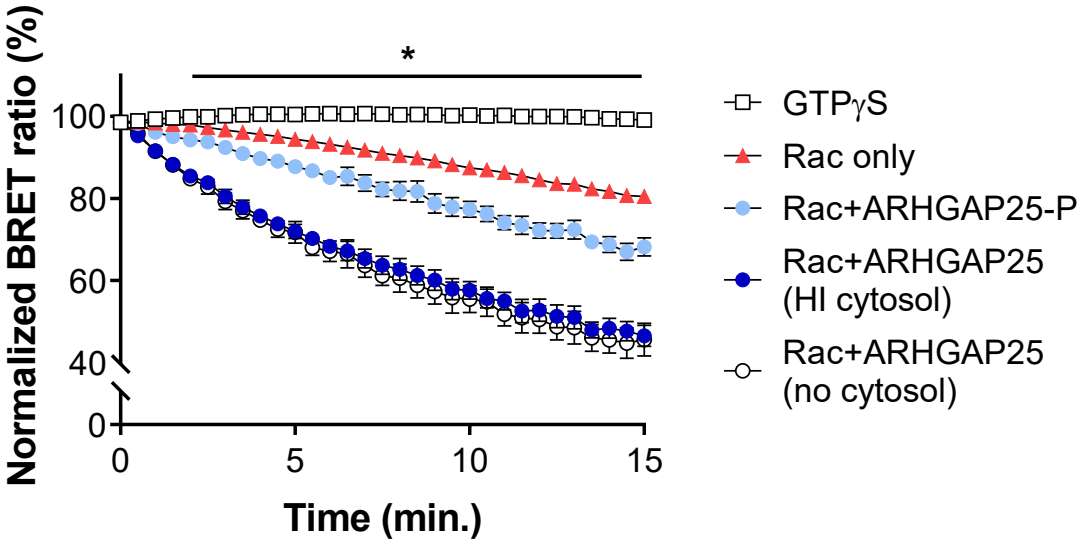

*Figure 35. Phosphorylated ARHGAP25 has a weaker GAP activity than the non-phosphorylated protein. There is virtually no difference between HI cytosol treatment and omitting cytosol altogether. Mean±SEM of 4 experiments is plotted. The lines above the diagrams show the significance of a from-to-interval; *p<0.05 Rac+ARHGAP25-P compared to Rac+ARHGAP25, two-way ANOVA followed by a Tukey post hoc test.*

The above results corroborated the previously measured effect of phosphorylation with the radioisotope method inasmuch as phosphorylation had an inhibitory effect on the GAP activity of ARHGAP25 (*cf.* ***Figures 22 and 36***).

DOI:10.14753/SE.2023.2903

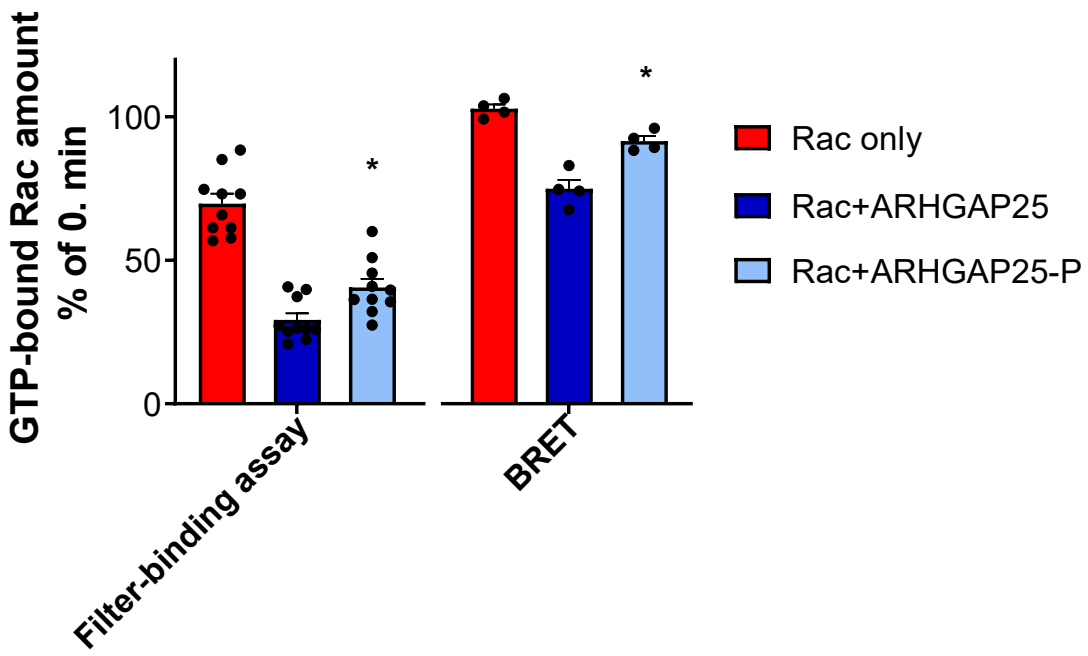

*Figure 36. Non-phosphorylated ARHGAP25 (Rac+ARHGAP25) increases Rac's endogenous GTPase activity (Rac only), while phosphorylated ARHGAP25 (Rac+ARHGAP25-P) has only a reduced effect on GAP activity. Data were obtained 5 min after ARHGAP25 addition. *p<0.05 Rac+ARHGAP25-P compared to Rac+ARHGAP25, two-way ANOVA. Mean+SEM of four (BRET) or ten (filter-binding assay) biological replicates is shown.*

Prominently, eliminating the phosphate groups in ARHGAP25 with an additional lambda protein phosphatase (LPP) treatment fully restored its GAP activity (***Figure 37***), implying the exclusive role of phosphorylation in the observed GAP activity change.

DOI:10.14753/SE.2023.2903

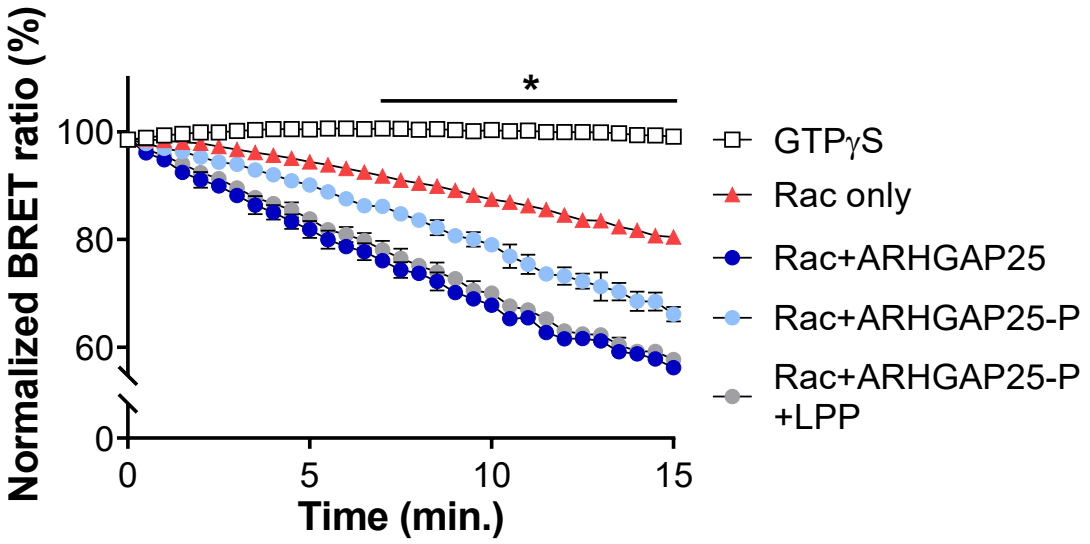

*Figure 37. Phosphorylation of ARHGAP25 weakens its GAP activity, which effect can be reversed with lambda phosphatase (LPP) treatment. 'Rac+ARHGAP25' corresponds to the protein incubated with heat-inactivated cytosol. *p<0.05 Rac+ARHGAP25-P compared to Rac+ARHGAP25-P+LPP, two-way ANOVA with Tukey post-hoc test. Mean±SEM of three independent experiments is shown.*

To further strengthen the notion that phosphorylation reduces the BRET ratio through weakening ARHGAP25's enzymatic activity, we worked with an enzymatically compromised ARHGAP25 mutant (described in (27)). In this construct, the highly conserved arginine R200 within the GAP domain is mutated, causing almost complete inhibition of the GAP activity *regardless* of the cytosol treatment (***Figure 38***). (Complete inhibition was not achieved, presumably because additional residues are also involved in the interaction between small GTPases and their GAPs and can contribute to the catalytic process (12).)

DOI:10.14753/SE.2023.2903

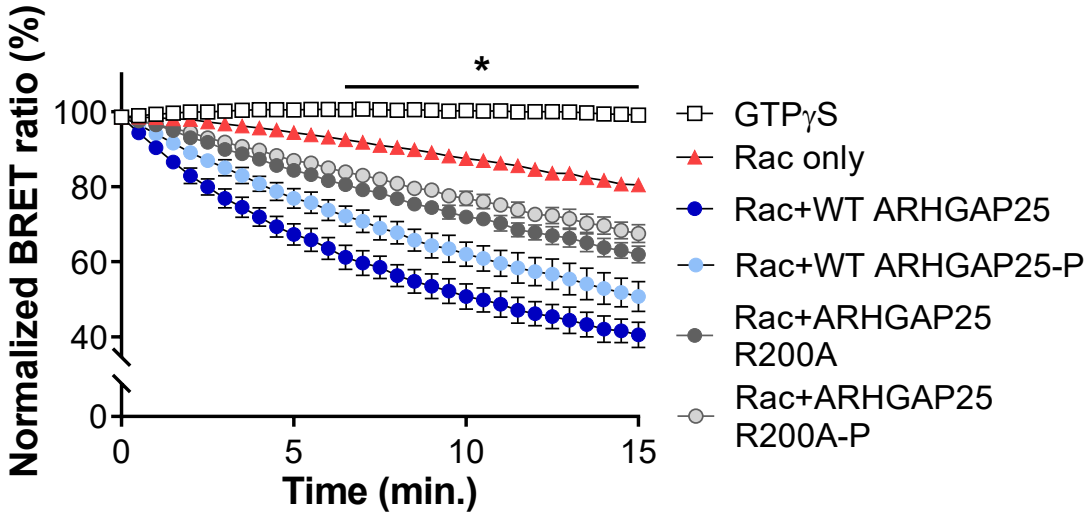

*Figure 38. Unlike the wild-type protein, the enzymatically defective R200A ARHGAP25 mutant shows a weakened GAP activity regardless of the phosphorylation state. Mean±SEM of three independent experiments is shown. *p<0.05 Rac+WT ARHGAP25-P compared to Rac+WT ARHGAP25, two-way ANOVA.*

5.3 ARHGAP25's GAP activity depends on S363 and S488, but not S379-380 phosphorylation

At last, we examined the effect of the three serine mutations on ARHGAP25's GAP activity and its sensitivity to phosphorylation. Like that observed with the radioisotope method, mutation of S363 to alanine completely abolished the inhibitory effect of phosphorylation on ARHGAP25's RacGAP activity compared to WT (***Figure 39B***). S488A mutant acted similarly to S363A: RacGAP activity did not differ from the non-phosphorylated form after neutrophil cytosol treatment (***Figure 39D***), suggesting that phosphorylation of these two residues is necessary for the inhibitory effect on ARHGAP25's RacGAP activity. Interestingly, mutation of serine residues at positions 379 and 380 (S379-380A) showed an altered phenotype compared to the previous mutants as phosphorylation caused a significant inhibition of ARHGAP25's RacGAP activity similar to that observed with the wild type protein (***Figure 39C***).

DOI:10.14753/SE.2023.2903

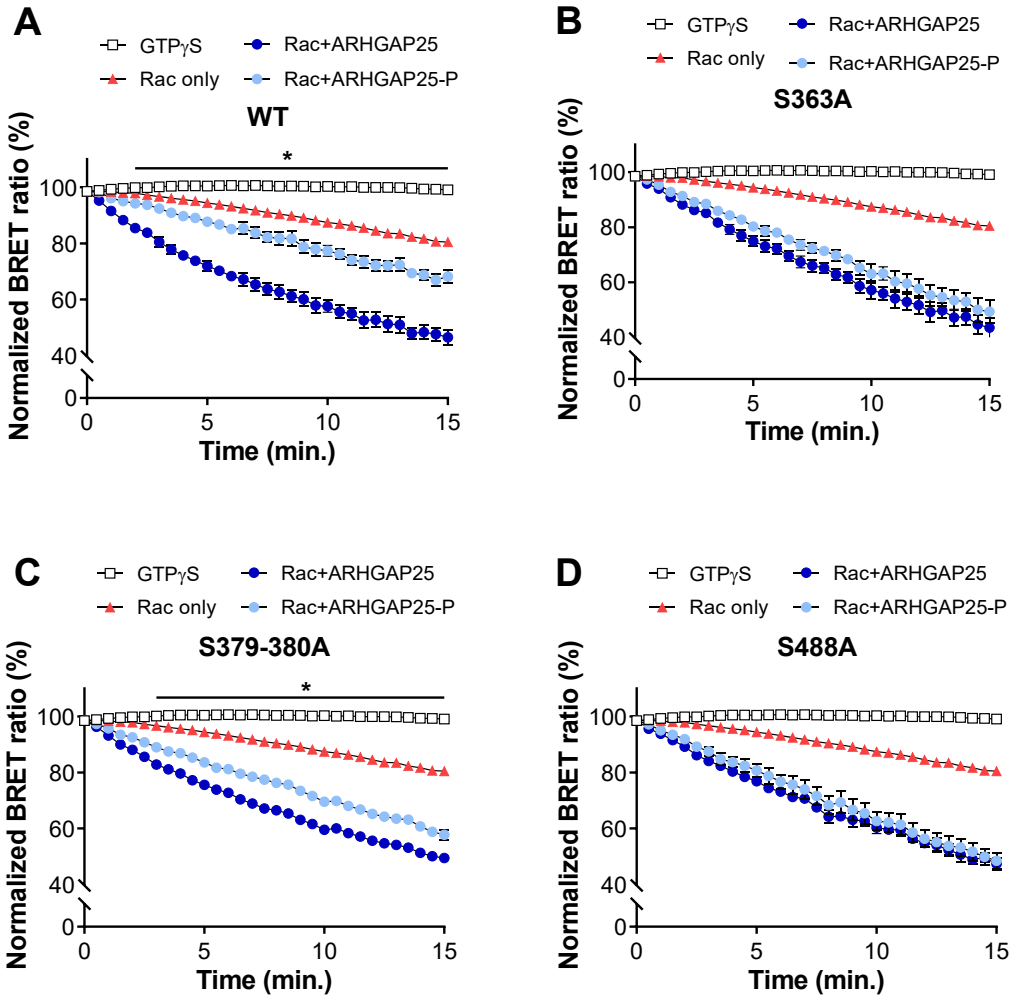

*Figure 39. Effect of phosphorylation-deficient (Ser-to-Ala) mutations on the GAP activity of ARHGAP25. Wild type and mutant ARHGAP25 constructs were pre-treated with neutrophil cytosol (intact or heat-inactivated, referred to as ARHGAP25-P and ARHGAP25, respectively) for 30 minutes and then added to Venus-Rac and CRIB-RLuc. Mean±SEM of four (A; D) or five (B; C) independent experiments is plotted. Regarding Rac and GTPγS, the mean±SEM of 50 independent experiments (biological replicates) is shown. The lines above the diagrams show the significance of a from-to-interval. *p<0.05 Rac+ARHGAP25-P compared to Rac+ARHGAP25, two-way ANOVA followed by a Tukey post hoc test.*

Investigation of double-mutant ARHGAP25 proteins painted a more nuanced picture of their role. Double S-A mutations of S363+S488, S379-380A+S488A and S363A+S379-380A almost completely abolished the sensitivity of ARGAP25`s GAP activity to

DOI:10.14753/SE.2023.2903

phosphorylation, with the S363A+S379-380A mutant retaining some sensitivity. However, surprisingly, triple mutation ARHGAP25 (S363A+S379-380A+S488A) restored this sensitivity to phosphorylation (***Figure 40***). These observations suggest that mutations of S379 and/or S380 may have a more specialized effect and are not directly involved in inhibiting ARHGAP25's RacGAP activity by phosphorylation.

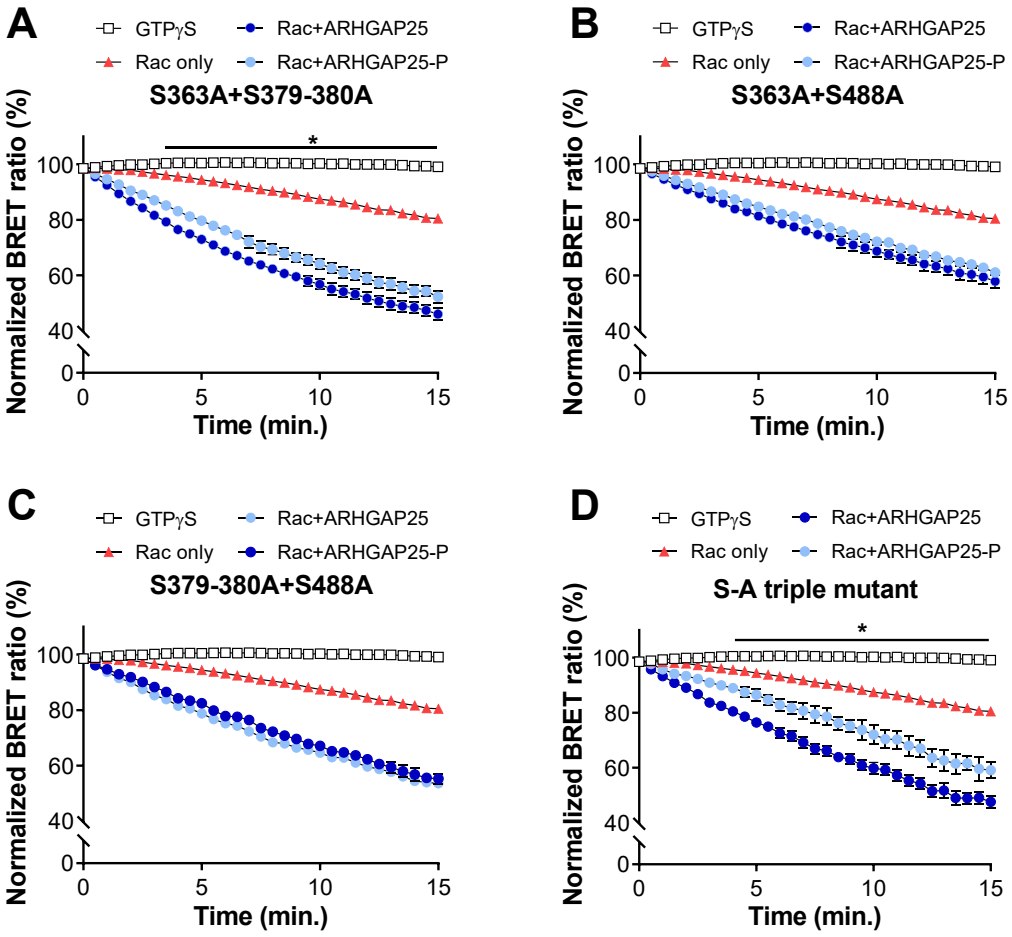

Figure 40. Effect of phosphorylation-deficient (Ser-to-Ala) mutations on the GAP activity of ARHGAP25. Wild type and mutant ARHGAP25 constructs were pre-treated with neutrophil cytosol (intact or heat-inactivated, referred to as ARHGAP25-P and ARHGAP25, resp.) for 30 minutes and then added to Venus-Rac and CRIB-Rluc. Mean±SEM of four (B; C; D) or eight (A) independent experiments is plotted. Regarding Rac and GTPγS, the mean±SEM of 50 independent experiments (biological replicates) is shown. The lines above the diagrams show the significance of a from-to-interval. Data

*were analyzed using two-way ANOVA followed by a Tukey post hoc test. *p<0.05 Rac+ARHGAP25-P compared to Rac+ARHGAP25.*

For better comparison, we calculated decay rates from normalized BRET ratio data by fitting regression lines on the initial, two-minute linear section of the curves. This analysis confirmed our conclusions drawn from the above-shown kinetic curves (***Figure 41***).

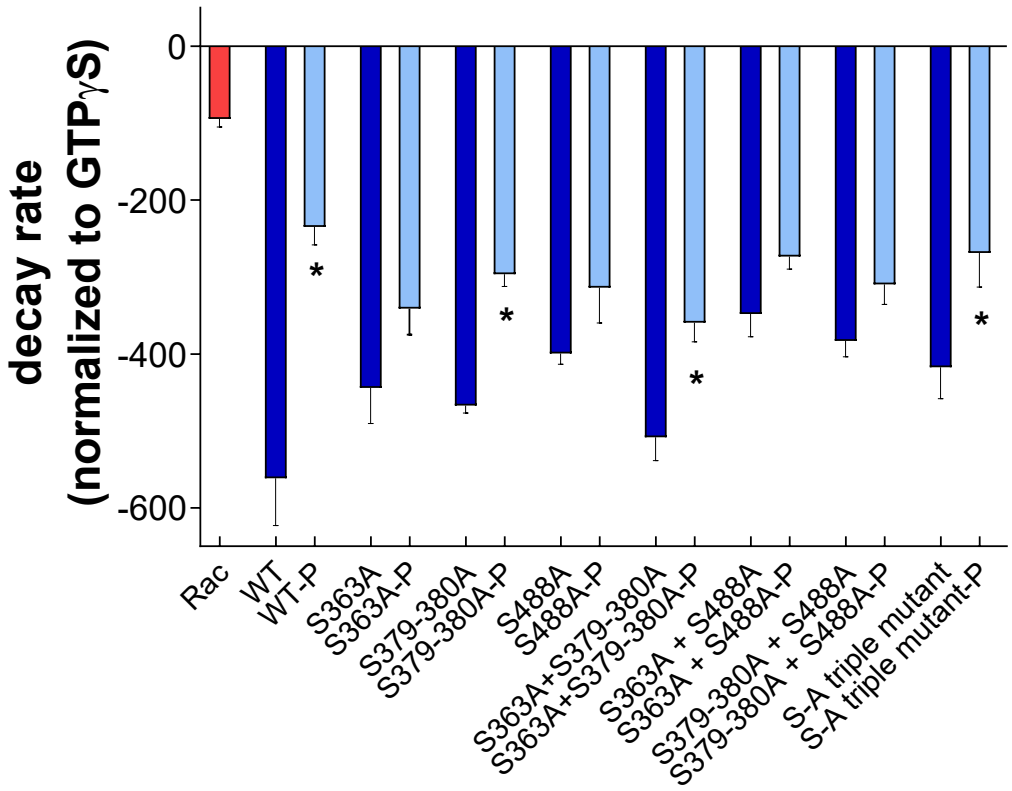

*Figure 41. The decay rates in the first two minutes of measurements shown in Figures 39 and 40 were calculated and plotted (normalized to GTPγS). Mean+SEM is shown, *p<0.05 ARHGAP25-P compared to ARHGAP25, unpaired t-tests.*

DOI:10.14753/SE.2023.2903

6. DISCUSSION

Rho family GTPases and their regulating proteins (GAPs, GEFs and GDIs) govern the actin-cytoskeleton organization, thereby modulating a plethora of biological processes such as migration, focal adhesions, cell polarity and diverse immunological tasks (19-21). Our research group was the first to characterize a novel GTPase activating protein of the Rho family, ARHGAP25. We examined its small G protein specificity and described its complex role in regulating leukocyte functions, including phagocytosis, superoxide production, and transmigration (26, 27, 51, 52). In addition, the role of ARHGAP25 in tumor cell metastasis has also recently been recognized (45, 46, 48, 50, 99, 100). However, despite its emerging immunological and oncological importance, the post-translational control of ARHGAP25 is almost entirely unknown, prompting us to explore this protein's regulation further.

We revealed that neutrophilic granulocyte kinases could phosphorylate ARHGAP25 under *in vitro* and *in vivo* conditions, and the phosphorylation is located mainly in the interdomain region. Furthermore, detailed mass spectrometry (MS) and *in silico* analysis narrowed the number of likely phosphoresidues to eleven.

In collaboration with Dr. Wang's group (Boston, MA, USA), we demonstrated that phosphorylation of serine 363 regulates the GAP activity of ARHGAP25 and thereby modulates the mobilization of hematopoietic stem cells and progenitor cells (HSPCs) from murine bone marrow (55). This study also suggested the functional importance of S379-380 and S488; therefore, we generated appropriate phosphodeletion (serine-to-alanine) mutants and examined the role of these residues on ARHGAP25's GAP activity.

To monitor the GAP activity of ARHGAP25 in a less labor-intensive manner that provides higher temporal resolution than currently available techniques, we first developed an *in vitro*, bioluminescence resonance energy transfer (BRET)-based GAP assay. In our method, the luciferase-tagged CRIB domain of p21-activated kinase (PAK) exclusively binds active Rac and excites the linked Venus protein so that we can infer the active Rac amount from the emission (BRET) ratio continuously.

We chose a cell-free assay because ARHGAP25's phosphorylation can be carried out more reliably this way, easily changing the concentrations in the reaction. In addition, we needed the simultaneous presence of three proteins (CRIB-RLuc, Venus-Rac,

ARHGAP25), sometimes even in different proportions (e.g., ARHGAP25 dose-dependency), which could be problematic when transfecting living cells. Advantages of this technique compared to other widely used *in vitro* methods, such as radioisotope-based GAP-assay or GTPase-Glo™ Assay, are: i) 96-well plates provide a higher number of samples and parallel experiments with every run; ii) radioisotope-labeling is not needed rendering the method safer and more cost-effective; iii) close-to real-time temporal resolution is achievable. Moreover, BRET does not suffer from issues often associated with FRET, such as autofluorescence, light scattering, or photobleaching. In fact, in high throughput assays, it has even higher sensitivity than FRET (101). Still, BRET was never used for GTPase measurements until now.

We verified that the BRET-based method has comparable sensitivity to other established GAP assays and still provides low variability. After ascertaining our BRET-GAP assay, we applied it to confirm that S363 indeed regulates the GAP activity of ARHGAP25, similarly to that observed with the radioisotope filter binding assay. Additionally, we revealed that the serine residue at position 488 also significantly impacts the RacGAP activity of ARHGAP25; phosphorylation of these two serines (S363, S488) inhibits the *in vitro* RacGAP activity of ARHGAP25. Moreover, RacGAP activity was independent of phosphorylation at S379-380, implying that modification at distinct residues may have a specific effect on ARHGAP25 protein function. As opposed to phosphorylation on S363A and/or S488A, phosphorylation of the S363A+S379-380A+S488A triple mutant ARHGAP25 with neutrophil cytosol *decreased* its RacGAP activity. Since our group has shown that ARHGAP25's membrane-binding capacity decreases after mutating all three serine residues (i.e., S363, S379-380, S488) but not with single or double mutation (102), we believe that phosphorylation can cause a negatively charged area which then modifies the protein-protein interactions (*e.g.*, the connection between ARHGAP25 and Rac), the structure, or even intramolecular interactions of ARHGAP25. A similar mechanism was described for p190RhoGAP in which the phosphorylation of the polybasic region altered the protein's small GTPase specificity and membrane binding (43).

We corroborated our *in vitro* observations by pull-down assays from resting and opsonized zymosan (OPZ)-stimulated neutrophilic PLB-985 cells. In these experiments, the S363A and S488A mutants, but not the S379-380A, showed decreased Rac activity upon stimulation compared to WT (102). Together, these data suggest a hypothesis that

the phosphorylation of ARHGAP25 during OPZ-evoked cell activation weakens its GAP activity resulting in more active Rac than in unstimulated cells. Conversely, if ARHGAP25 is not or cannot be phosphorylated on S363 or S488, it acts as a more effective GAP.

We also confirmed that, although phosphorylation of serine residues 363 and 488 had a clear inhibitory effect on ARHGAP25's GAP activity, mutation of these residues does not alter superoxide production in PLB-985 neutrophilic cells. In contrast, phosphorylation of serine residues 379 and 380, which did not affect GAP activity *in vitro*, was required for ARHGAP25's inhibitory effect on superoxide production (102). The apparent dissociation of ARHGAP25's GAP activity and its influence on superoxide production raises the possibility that the S379-380A mutant may alter the molecular interactions in the NADPH oxidase complex rather than affecting Rac's GTPase activity itself. Our research group previously demonstrated examples of these intermolecular interactions (26). These data suggest that phosphorylation of ARHGAP25 could regulate not only the GTPase activity of Rac but – in a steric manner – the interaction between Rac and $p67^{phox}$ (and maybe other GAPs, *e.g.*, p50RhoGAP) simultaneously.

Taken together, we present a new method for measuring GTPase/GAP activity by utilizing bioluminescence resonance energy transfer (BRET). Our data indicate that the RacGAP activity of ARHGAP25 is regulated directly by the phosphorylation of serine residues at positions 363 and/or 488 but not at 379-380 *in vitro.* We speculate that distinct phosphorylation patterns of ARHGAP25 result in specific functional states of this protein, similar to that described for heterotrimeric G-proteins ("barcode-dependent regulation") (103, 104).

DOI:10.14753/SE.2023.2903

7. CONCLUSIONS

According to the objectives and based on the above-described results, my conclusions are the following:

1. ARHGAP25, a Rac-specific GTPase activating protein with an essential role in neutrophilic granulocyte functions, can be phosphorylated by neutrophilic granulocyte cytosolic kinases.

2. Based on mass spectrometry data and *in silico* analysis, we identified eleven potential phosphorylation sites in ARHGAP25.

3. We developed a novel real-time bioluminescence resonance energy transfer (BRET) assay to monitor the GAP activity of ARHGAP25 *in vitro*.

4. Using both the radioactive filter-binding assay and our newly developed GTPase assay, we showed that ARHGAP25's phosphorylation weakens its enzymatic GAP activity under *in vitro* conditions.

5. Using phosphodeletion mutants, we revealed that phosphorylation of S363 and S488, but not that of S379-380, controls ARHGAP25's RacGAP activity.

DOI:10.14753/SE.2023.2903

8. SUMMARY

Small GTPases of the Rho family, such as Rac, Rho, and Cdc42, play an essential role in the actin-cytoskeleton organization, thereby regulating cell adhesion, migration, and immune cell responses. ARHGAP25, a Rac-specific GTPase activating protein, can accelerate Rac's slow, endogenous GTP hydrolysis and control its cyclic operation and effector functions. We previously described ARHGAP25's important role in phagocytosis, superoxide production, and transendothelial migration. Moreover, its complex role in tumor behavior has recently been recognized, rendering the post-translational modifications of ARHGAP25 all the more relevant.

During my Ph.D. studies, I examined ARHGAP25's phosphorylation and the effect of phosphorylation on its enzymatic GAP activity. We identified eleven phosphorylated amino acids using mass spectrometry and *in silico* database screening. In collaboration, we reported that phosphorylation occurs on serine 363 and plays a role in the mobilization of hematopoietic stem cells and progenitor cells (HPSCs) from murine bone marrow. The limitations of currently available GAP assays led us to develop a new, *in vitro* bioluminescence-resonance energy transfer (BRET)-based method, which utilizes the specific molecular interaction between Rac and CRIB, the latter capable of binding only the active, GTP-bound form of Rac. We verified that this new method has comparable sensitivity to other established GAP assays, and we could reproduce the data we obtained with the previously used filter-binding assay using radiolabeling. Our new approach proved to be a safer and cheaper alternative, providing high temporal resolution and simultaneously enabling the measurement of an increased number of samples. In addition, the BRET-based GAP assay allowed us to demonstrate that the phosphorylation of ARHGAP25 with neutrophil cytosol kinases mitigates its enzymatic activity. Using phosphodeletion (serine-to-alanine) mutants, we revealed the selective role of serine residues S363 and S488, but not S379-380, in the phosphorylation-dependent regulation of ARHGAP25's GAP activity.

DOI:10.14753/SE.2023.2903

9. ÖSSZEFOGLALÓ

A Rho családba tartozó ciklikus működésű kis G-fehérjék, úgymint Rho, Rac és Cdc42 az aktin-citoszkeleton rendszer szabályozásán keresztül olyan fontos sejtműködésekben vesznek részt, mint az adhézió, migráció és az immunsejtek effektor válaszai. A GTPáz aktiváló proteinek, más néven GAP-ok képesek a kis G-fehérjék lassú, endogén GTP hidrolízisét fokozni, ezzel elősegítve az inaktív, GDP-t kötött állapot létrejöttét. Munkacsoportunk elsőként írta le a Rac-specifikus ARHGAP25 szabályozó szerepét a neutrofil granulociták fagocitózisában, szuperoxid-termelésében és endotélen keresztüli vándorlásában. Az utóbbi években megszaporodott azon tanulmányok száma is, melyek az ARHGAP25 jelentőségét mutatták ki különböző, nem hemopoetikus sejt-eredetű daganatok kialakulásában és metasztázisában. Ez utóbbi még időszerűbbé teszi az ARHGAP25 (poszt-transzlációs) szabályozásának kutatását, melyről eddig kevés ismerettel rendelkezünk.

Ph.D. munkám során az ARHGAP25 foszforilációját vizsgáltam, valamint ennek hatását a fehérje enzimatikus működésére. Adatbázisok segítségével és tömegspektrometriai analízissel tizenegy foszforilációs helyet azonosítottunk az ARHGAP25 szerkezetén belül. Kollaborációs partnerünkkel megállapítottuk, hogy a 363. pozícióban levő szerin foszforilációja jelentős szerepet tölt be egerekben a hemopoetikus ős- és progenitor sejtek (HPSC) csontvelőből történő kivándorlásában. A jelenleg elérhető, az *in vitro* GAP aktivitás mérésére szolgáló módszerek korlátai és hátrányai miatt kifejlesztettünk egy bioluminescencia rezonancia energia transzfer (BRET) alapú módszert, mely a Rac és az őt aktív állapotban kötő CRIB domén kölcsönhatásán alapul. Igazoltuk, hogy módszerünk összemérhető más GAP próbákkal, és ezen felül költséghatékony, biztonságos (nincs szükség izotópra), kiváló időbeli felbontást nyújt, és nagy elemszámú minta vizsgálható vele. Kimutattuk, hogy a neutrofil granulociták citoszoljában található kinázok képesek foszforilálni az ARHGAP25-öt, és ezen foszforiláció gátolja a GAP aktivitást. Végül foszforilációra képtelen (szerin-alanin) mutánsok segítségével bizonyítottuk, hogy a GAP aktivitás gátlásában a 363. és 488. pozícióban levő szerinek foszforilációja jelentős szerepet játszik, míg a 379-380. szerinek foszforilációja nincs hatással az ARHGAP25 enzimaktivitására.

10. REFERENCES

1. Takai Y, Sasaki T, Matozaki T. (2001) Small GTP-binding proteins. Physiol Rev, 81: 153-208.
2. Wennerberg K, Rossman KL, Der CJ. (2005) The Ras superfamily at a glance. J Cell Sci, 118: 843-846.
3. Self AJ, Hall A. (1995) Measurement of intrinsic nucleotide exchange and GTP hydrolysis rates. Methods Enzymol, 256: 67-76.
4. Bos JL, Rehmann H, Wittinghofer A. (2007) GEFs and GAPs: critical elements in the control of small G proteins. Cell, 129: 865-877.
5. McEwen DP, Gee KR, Kang HC, Neubig RR. (2001) Fluorescent BODIPY-GTP analogs: real-time measurement of nucleotide binding to G proteins. Anal Biochem, 291: 109-117.
6. Csépányi-Kömi R, Lévay M, Ligeti E. (2012) Small G proteins and their regulators in cellular signalling. Mol Cell Endocrinol, 353: 10-20.
7. Csépányi-Kömi R, Pásztor M, Bartos B, Ligeti E. (2018) The neglected terminators: Rho family GAPs in neutrophils. Eur J Clin Invest, 48 Suppl 2: e12993.
8. Ligeti E, Welti S, Scheffzek K. (2012) Inhibition and termination of physiological responses by GTPase activating proteins. Physiol Rev, 92: 237-272.
9. Bourne HR, Sanders DA, McCormick F. (1991) The GTPase superfamily: conserved structure and molecular mechanism. Nature, 349: 117-127.
10. Vetter IR, Wittinghofer A. (2001) The guanine nucleotide-binding switch in three dimensions. Science, 294: 1299-1304.
11. Gasper R, Wittinghofer F. (2019) The Ras switch in structural and historical perspective. Biol Chem, 401: 143-163.
12. Scheffzek K, Ahmadian MR, Kabsch W, Wiesmüller L, Lautwein A, Schmitz F, Wittinghofer A. (1997) The Ras-RasGAP complex: structural basis for GTPase activation and its loss in oncogenic Ras mutants. Science, 277: 333-338.
13. Rittinger K, Walker PA, Eccleston JF, Nurmahomed K, Owen D, Laue E, Gamblin SJ, Smerdon SJ. (1997) Crystal structure of a small G protein in complex with the GTPase-activating protein rhoGAP. Nature, 388: 693-697.

14. Pan X, Eathiraj S, Munson M, Lambright DG. (2006) TBC-domain GAPs for Rab GTPases accelerate GTP hydrolysis by a dual-finger mechanism. Nature, 442: 303-306.
15. Daumke O, Weyand M, Chakrabarti PP, Vetter IR, Wittinghofer A. (2004) The GTPase-activating protein Rap1GAP uses a catalytic asparagine. Nature, 429: 197-201.
16. Scheffzek K, Ahmadian MR. (2005) GTPase activating proteins: structural and functional insights 18 years after discovery. Cell Mol Life Sci, 62: 3014-3038.
17. Boureux A, Vignal E, Faure S, Fort P. (2007) Evolution of the Rho family of ras-like GTPases in eukaryotes. Mol Biol Evol, 24: 203-216.
18. Wang T, Rao D, Yu C, Sheng J, Luo Y, Xia L, Huang W. (2022) RHO GTPase family in hepatocellular carcinoma. Exp Hematol Oncol, 11: 91.
19. Hall A. (1998) G proteins and small GTPases: distant relatives keep in touch. Science, 280: 2074-2075.
20. Ridley AJ. (2006) Rho GTPases and actin dynamics in membrane protrusions and vesicle trafficking. Trends Cell Biol, 16: 522-529.
21. Bokoch GM. (2005) Regulation of innate immunity by Rho GTPases. Trends Cell Biol, 15: 163-171.
22. Csépányi-Kömi R, Sáfár D, Grósz V, Tarján ZL, Ligeti E. (2013) In silico tissue-distribution of human Rho family GTPase activating proteins. Small GTPases, 4: 90-101.
23. Csépányi-Kömi R, Lévay M, Ligeti E. (2012) Rho/RacGAPs: embarras de richesse? Small GTPases, 3: 178-182.
24. Brouns MR, Matheson SF, Hu KQ, Delalle I, Caviness VS, Silver J, Bronson RT, Settleman J. (2000) The adhesion signaling molecule p190 RhoGAP is required for morphogenetic processes in neural development. Development, 127: 4891-4903.
25. Lahoz A, Hall A. (2008) DLC1: a significant GAP in the cancer genome. Genes Dev, 22: 1724-1730.
26. Lőrincz Á M, Szarvas G, Smith SM, Ligeti E. (2014) Role of Rac GTPase activating proteins in regulation of NADPH oxidase in human neutrophils. Free Radic Biol Med, 68: 65-71.

27. Csépányi-Kömi R, Sirokmány G, Geiszt M, Ligeti E. (2012) ARHGAP25, a novel Rac GTPase-activating protein, regulates phagocytosis in human neutrophilic granulocytes. Blood, 119: 573-582.
28. Um K, Niu S, Duman JG, Cheng JX, Tu YK, Schwechter B, Liu F, Hiles L, Narayanan AS, Ash RT, Mulherkar S, Alpadi K, Smirnakis SM, Tolias KF. (2014) Dynamic control of excitatory synapse development by a Rac1 GEF/GAP regulatory complex. Dev Cell, 29: 701-715.
29. Smith LE, Rogowska-Wrzesinska A. (2020) The challenge of detecting modifications on proteins. Essays Biochem, 64: 135-153.
30. Farooq A, Bhat KA, Mir RA, Mahajan R, Nazir M, Sharma V, Zargar SM. (2022) Emerging trends in developing biosensor techniques to undertake plant phosphoproteomic analysis. J Proteomics, 253: 104458.
31. de Oliveira PS, Ferraz FA, Pena DA, Pramio DT, Morais FA, Schechtman D. (2016) Revisiting protein kinase-substrate interactions: Toward therapeutic development. Sci Signal, 9: re3.
32. Ardito F, Giuliani M, Perrone D, Troiano G, Lo Muzio L. (2017) The crucial role of protein phosphorylation in cell signaling and its use as targeted therapy (Review). Int J Mol Med, 40: 271-280.
33. Jin J, Pawson T. (2012) Modular evolution of phosphorylation-based signalling systems. Philos Trans R Soc Lond B Biol Sci, 367: 2540-2555.
34. Minoshima Y, Kawashima T, Hirose K, Tonozuka Y, Kawajiri A, Bao YC, Deng X, Tatsuka M, Narumiya S, May WS, Jr., Nosaka T, Semba K, Inoue T, Satoh T, Inagaki M, Kitamura T. (2003) Phosphorylation by aurora B converts MgcRacGAP to a RhoGAP during cytokinesis. Dev Cell, 4: 549-560.
35. Touré A, Mzali R, Liot C, Seguin L, Morin L, Crouin C, Chen-Yang I, Tsay YG, Dorseuil O, Gacon G, Bertoglio J. (2008) Phosphoregulation of MgcRacGAP in mitosis involves Aurora B and Cdk1 protein kinases and the PP2A phosphatase. FEBS Lett, 582: 1182-1188.
36. I ST, Nie Z, Stewart A, Najdovska M, Hall NE, He H, Randazzo PA, Lock P. (2004) ARAP3 is transiently tyrosine phosphorylated in cells attaching to fibronectin and inhibits cell spreading in a RhoGAP-dependent manner. J Cell Sci, 117: 6071-6084.

37. Sordella R, Jiang W, Chen GC, Curto M, Settleman J. (2003) Modulation of Rho GTPase signaling regulates a switch between adipogenesis and myogenesis. Cell, 113: 147-158.
38. Caron C, DeGeer J, Fournier P, Duquette PM, Luangrath V, Ishii H, Karimzadeh F, Lamarche-Vane N, Royal I. (2016) CdGAP/ARHGAP31, a Cdc42/Rac1 GTPase regulator, is critical for vascular development and VEGF-mediated angiogenesis. Sci Rep, 6: 27485.
39. He Y, Northey JJ, Primeau M, Machado RD, Trembath R, Siegel PM, Lamarche-Vane N. (2011) CdGAP is required for transforming growth factor β- and Neu/ErbB-2-induced breast cancer cell motility and invasion. Oncogene, 30: 1032-1045.
40. Ben Djoudi Ouadda A, He Y, Calabrese V, Ishii H, Chidiac R, Gratton JP, Roux PP, Lamarche-Vane N. (2018) CdGAP/ARHGAP31 is regulated by RSK phosphorylation and binding to 14-3-3β adaptor protein. Oncotarget, 9: 11646-11664.
41. Ohta Y, Hartwig JH, Stossel TP. (2006) FilGAP, a Rho- and ROCK-regulated GAP for Rac binds filamin A to control actin remodelling. Nat Cell Biol, 8: 803-814.
42. Morishita Y, Tsutsumi K, Ohta Y. (2015) Phosphorylation of Serine 402 Regulates RacGAP Protein Activity of FilGAP Protein. J Biol Chem, 290: 26328-26338.
43. Lévay M, Settleman J, Ligeti E. (2009) Regulation of the substrate preference of p190RhoGAP by protein kinase C-mediated phosphorylation of a phospholipid binding site. Biochemistry, 48: 8615-8623.
44. Katoh M, Katoh M. (2004) Identification and characterization of ARHGAP24 and ARHGAP25 genes in silico. Int J Mol Med, 14: 333-338.
45. Thuault S, Comunale F, Hasna J, Fortier M, Planchon D, Elarouci N, De Reynies A, Bodin S, Blangy A, Gauthier-Rouvière C. (2016) The RhoE/ROCK/ARHGAP25 signaling pathway controls cell invasion by inhibition of Rac activity. Mol Biol Cell, 27: 2653-2661.
46. Xu K, Liu B, Ma Y. (2019) The tumor suppressive roles of ARHGAP25 in lung cancer cells. Onco Targets Ther, 12: 6699-6710.

47. Shi F, Wu J, Jia Q, Li K, Li W, Shi Y, Wang Y, Wu S. (2022) Relationship between the expression of ARHGAP25 and RhoA in non-small cell lung cancer and vasculogenic mimicry. BMC Pulm Med, 22: 377.
48. Tao L, Zhu Y, Gu Y, Zheng J, Yang J. (2019) ARHGAP25: A negative regulator of colorectal cancer (CRC) metastasis via the Wnt/β-catenin pathway. Eur J Pharmacol, 858: 172476.
49. Zhang Y, Lin Y, Zhu Y, Zhang X, Tao L, Yang M. (2022) ARHGAP25 expression in colorectal cancer as a biomarker associated with favorable prognosis. Mol Clin Oncol, 16: 84.
50. Huang WK, Chen Y, Su H, Chen TY, Gao J, Liu Y, Yeh CN, Li S. (2021) ARHGAP25 Inhibits Pancreatic Adenocarcinoma Growth by Suppressing Glycolysis via AKT/mTOR Pathway. Int J Biol Sci, 17: 1808-1820.
51. Schlam D, Bagshaw RD, Freeman SA, Collins RF, Pawson T, Fairn GD, Grinstein S. (2015) Phosphoinositide 3-kinase enables phagocytosis of large particles by terminating actin assembly through Rac/Cdc42 GTPase-activating proteins. Nat Commun, 6: 8623.
52. Csépányi-Kömi R, Wisniewski É, Bartos B, Lévai P, Németh T, Balázs B, Kurz AR, Bierschenk S, Sperandio M, Ligeti E. (2016) Rac GTPase Activating Protein ARHGAP25 Regulates Leukocyte Transendothelial Migration in Mice. J Immunol, 197: 2807-2815.
53. Lindner SE, Egelston CA, Huard SM, Lee PP, Wang LD. (2020) Arhgap25 Deficiency Leads to Decreased Numbers of Peripheral Blood B Cells and Defective Germinal Center Reactions. Immunohorizons, 4: 274-281.
54. Xiao H, Wang G, Zhao M, Shuai W, Ouyang L, Sun Q. (2023) Ras superfamily GTPase activating proteins in cancer: Potential therapeutic targets? Eur J Med Chem, 248: 115104.
55. Wang LD, Ficarro SB, Hutchinson JN, Csepanyi-Komi R, Nguyen PT, Wisniewski E, Sullivan J, Hofmann O, Ligeti E, Marto JA, Wagers AJ. (2016) Phosphoproteomic profiling of mouse primary HSPCs reveals new regulators of HSPC mobilization. Blood, 128: 1465-1474.

56. Tan TJ, Vollmer P, Gallwitz D. (1991) Identification and partial purification of GTPase-activating proteins from yeast and mammalian cells that preferentially act on Ypt1/Rab1 proteins. FEBS Lett, 291: 322-326.
57. Kanie T, Jackson PK. (2018) Guanine Nucleotide Exchange Assay Using Fluorescent MANT-GDP. Bio Protoc, 8.
58. Hiratsuka T. (1983) New ribose-modified fluorescent analogs of adenine and guanine nucleotides available as substrates for various enzymes. Biochim Biophys Acta, 742: 496-508.
59. John J, Sohmen R, Feuerstein J, Linke R, Wittinghofer A, Goody RS. (1990) Kinetics of interaction of nucleotides with nucleotide-free H-ras p21. Biochemistry, 29: 6058-6065.
60. Gureasko J, Galush WJ, Boykevisch S, Sondermann H, Bar-Sagi D, Groves JT, Kuriyan J. (2008) Membrane-dependent signal integration by the Ras activator Son of sevenless. Nat Struct Mol Biol, 15: 452-461.
61. Sondermann H, Soisson SM, Boykevisch S, Yang SS, Bar-Sagi D, Kuriyan J. (2004) Structural analysis of autoinhibition in the Ras activator Son of sevenless. Cell, 119: 393-405.
62. Blaise AM, Corcoran EE, Wattenberg ES, Zhang Y-L, Cottrell JR, Koleske AJ. (2021) In vitro fluorescence assay to measure GDP/GTP exchange of guanine nucleotide exchange factors of Rho family GTPases. Biology Methods and Protocols, 7.
63. Eccleston JF, Moore KJ, Morgan L, Skinner RH, Lowe PN. (1993) Kinetics of interaction between normal and proline 12 Ras and the GTPase-activating proteins, p120-GAP and neurofibromin. The significance of the intrinsic GTPase rate in determining the transforming ability of ras. J Biol Chem, 268: 27012-27019.
64. Sermon BA, Lowe PN, Strom M, Eccleston JF. (1998) The importance of two conserved arginine residues for catalysis by the ras GTPase-activating protein, neurofibromin. J Biol Chem, 273: 9480-9485.
65. Phillips RA, Hunter JL, Eccleston JF, Webb MR. (2003) The mechanism of Ras GTPase activation by neurofibromin. Biochemistry, 42: 3956-3965.

66. Mazhab-Jafari MT, Marshall CB, Smith M, Gasmi-Seabrook GM, Stambolic V, Rottapel R, Neel BG, Ikura M. (2010) Real-time NMR study of three small GTPases reveals that fluorescent 2'(3')-O-(N-methylanthraniloyl)-tagged nucleotides alter hydrolysis and exchange kinetics. J Biol Chem, 285: 5132-5136.
67. Kraemer A, Brinkmann T, Plettner I, Goody R, Wittinghofer A. (2002) Fluorescently labelled guanine nucleotide binding proteins to analyse elementary steps of GAP-catalysed reactions. J Mol Biol, 324: 763-774.
68. Eberth A, Dvorsky R, Becker CF, Beste A, Goody RS, Ahmadian MR. (2005) Monitoring the real-time kinetics of the hydrolysis reaction of guanine nucleotide-binding proteins. Biol Chem, 386: 1105-1114.
69. Mondal S, Hsiao K, Goueli SA. (2015) A Homogenous Bioluminescent System for Measuring GTPase, GTPase Activating Protein, and Guanine Nucleotide Exchange Factor Activities. Assay Drug Dev Technol, 13: 444-455.
70. Promega. https://www.promega.com/products/cell-signaling/gpcr-signaling/gtpase-glo-assay/?catNum=V7681#protocols.
71. BellBrook. https://www.bellbrooklabs.com/gdp-gap-assay/.
72. Webb MR. (1992) A continuous spectrophotometric assay for inorganic phosphate and for measuring phosphate release kinetics in biological systems. Proc Natl Acad Sci U S A, 89: 4884-4887.
73. Bishop AL, Hall A. (2000) Rho GTPases and their effector proteins. Biochem J, 348 Pt 2: 241-255.
74. Thompson G, Owen D, Chalk PA, Lowe PN. (1998) Delineation of the Cdc42/Rac-binding domain of p21-activated kinase. Biochemistry, 37: 7885-7891.
75. Benard V, Bokoch GM. (2002) Assay of Cdc42, Rac, and Rho GTPase activation by affinity methods. Methods Enzymol, 345: 349-359.
76. Ren XD, Schwartz MA. (2000) Determination of GTP loading on Rho. Methods Enzymol, 325: 264-272.
77. Nottingham RM, Pfeffer SR. (2015) Measuring Rab GTPase-activating protein (GAP) activity in live cells and extracts. Methods Mol Biol, 1298: 61-71.

78. Ozawa T, Kaihara A, Sato M, Tachihara K, Umezawa Y. (2001) Split luciferase as an optical probe for detecting protein-protein interactions in mammalian cells based on protein splicing. Anal Chem, 73: 2516-2521.
79. Anderson EL, Hamann MJ. (2012) Detection of Rho GEF and GAP activity through a sensitive split luciferase assay system. Biochem J, 441: 869-879.
80. Leng W, Pang X, Xia H, Li M, Chen L, Tang Q, Yuan D, Li R, Li L, Gao F, Bi F. (2013) Novel split-luciferase-based genetically encoded biosensors for noninvasive visualization of Rho GTPases. PLoS One, 8: e62230.
81. Pollok BA, Heim R. (1999) Using GFP in FRET-based applications. Trends Cell Biol, 9: 57-60.
82. Stryer L. (1978) Fluorescence energy transfer as a spectroscopic ruler. Annu Rev Biochem, 47: 819-846.
83. Miyawaki A. (2003) Visualization of the spatial and temporal dynamics of intracellular signaling. Dev Cell, 4: 295-305.
84. Kraynov VS, Chamberlain C, Bokoch GM, Schwartz MA, Slabaugh S, Hahn KM. (2000) Localized Rac activation dynamics visualized in living cells. Science, 290: 333-337.
85. Mochizuki N, Yamashita S, Kurokawa K, Ohba Y, Nagai T, Miyawaki A, Matsuda M. (2001) Spatio-temporal images of growth-factor-induced activation of Ras and Rap1. Nature, 411: 1065-1068.
86. Komatsu N, Aoki K, Yamada M, Yukinaga H, Fujita Y, Kamioka Y, Matsuda M. (2011) Development of an optimized backbone of FRET biosensors for kinases and GTPases. Mol Biol Cell, 22: 4647-4656.
87. Wong HL, Akamatsu A, Wang Q, Higuchi M, Matsuda T, Okuda J, Kosami KI, Inada N, Kawasaki T, Kaneko-Kawano T, Nagawa S, Tan L, Kawano Y, Shimamoto K. (2018) In vivo monitoring of plant small GTPase activation using a Förster resonance energy transfer biosensor. Plant Methods, 14: 56.
88. Phillips GN, Jr. (1997) Structure and dynamics of green fluorescent protein. Curr Opin Struct Biol, 7: 821-827.
89. Graham DL, Lowe PN, Chalk PA. (2001) A method to measure the interaction of Rac/Cdc42 with their binding partners using fluorescence resonance energy

transfer between mutants of green fluorescent protein. Anal Biochem, 296: 208-217.

90. Aoki K, Kiyokawa E, Nakamura T, Matsuda M. (2008) Visualization of growth signal transduction cascades in living cells with genetically encoded probes based on Förster resonance energy transfer. Philos Trans R Soc Lond B Biol Sci, 363: 2143-2151.
91. Azad T, Tashakor A, Hosseinkhani S. (2014) Split-luciferase complementary assay: applications, recent developments, and future perspectives. Anal Bioanal Chem, 406: 5541-5560.
92. Goody PR. (2016) Intrinsic protein fluorescence assays for GEF, GAP and post-translational modifications of small GTPases. Anal Biochem, 515: 22-25.
93. Fidyk NJ, Cerione RA. (2002) Understanding the catalytic mechanism of GTPase-activating proteins: demonstration of the importance of switch domain stabilization in the stimulation of GTP hydrolysis. Biochemistry, 41: 15644-15653.
94. Rada BK, Geiszt M, Káldi K, Timár C, Ligeti E. (2004) Dual role of phagocytic NADPH oxidase in bacterial killing. Blood, 104: 2947-2953.
95. Paulmurugan R, Gambhir SS. (2003) Monitoring protein-protein interactions using split synthetic renilla luciferase protein-fragment-assisted complementation. Anal Chem, 75: 1584-1589.
96. Xu X, Barry DC, Settleman J, Schwartz MA, Bokoch GM. (1994) Differing structural requirements for GTPase-activating protein responsiveness and NADPH oxidase activation by Rac. J Biol Chem, 269: 23569-23574.
97. Kozma R, Ahmed S, Best A, Lim L. (1996) The GTPase-activating protein n-chimaerin cooperates with Rac1 and Cdc42Hs to induce the formation of lamellipodia and filopodia. Mol Cell Biol, 16: 5069-5080.
98. Traut TW. (1994) Physiological concentrations of purines and pyrimidines. Mol Cell Biochem, 140: 1-22.
99. Tao L, Gu Y, Zheng J, Yang J, Zhu Y. (2019) Weichang'an suppressed migration and invasion of HCT116 cells by inhibiting Wnt/β-catenin pathway while upregulating ARHGAP25. Biotechnol Appl Biochem, 66: 787-793.

100. Ding FP, Tian JY, Wu J, Han DF, Zhao D. (2021) Identification of key genes as predictive biomarkers for osteosarcoma metastasis using translational bioinformatics. Cancer Cell Int, 21: 640.
101. Boute N, Jockers R, Issad T. (2002) The use of resonance energy transfer in high-throughput screening: BRET versus FRET. Trends Pharmacol Sci, 23: 351-354.
102. Wisniewski É, Czárán D, Kovács F, Bahurek E, Németh A, Sasvári P, Szanda G, Pettkó-Szandtner A, Klement E, Ligeti E, Csépányi-Kömi R. (2022) A novel BRET-Based GAP assay reveals phosphorylation-dependent regulation of the RAC-specific GTPase activating protein ARHGAP25. Faseb j, 36: e22584.
103. Flock T, Hauser AS, Lund N, Gloriam DE, Balaji S, Babu MM. (2017) Selectivity determinants of GPCR-G-protein binding. Nature, 545: 317-322.
104. Kaya AI, Perry NA, Gurevich VV, Iverson TM. (2020) Phosphorylation barcode-dependent signal bias of the dopamine D1 receptor. Proc Natl Acad Sci U S A, 117: 14139-14149.

11. BIBLIOGRAPHY OF THE CANDIDATE'S PUBLICATIONS

Candidate's publications related to the work discussed in this thesis

Wisniewski, Éva ; Czárán, Domonkos* ; Kovács, Fanni ; Bahurek, Enikő ; Németh, Afrodité ; Sasvári, Péter ; Szanda, Gergő ; Pettkó-Szandtner, Aladár ; Klement, Eva ; Ligeti, Erzsébet et al.
A Novel BRET-Based GAP Assay Reveals Phosphorylation-Dependent Regulation of the RAC-specific GTPase activating protein ARHGAP25
FASEB JOURNAL 36 : 11 Paper: e22584 , 19 p. (2022)
*Éva Wisniewski and Domonkos Czárán should be considered joint first authors.
IF: 5,834
DOI: 10.1096/fj.202200689R

Wang, LD ; Ficarro, SB ; Hutchinson, JN ; Csepanyi-Komi, R ; Nguyen, PT ; **Wisniewski, E** ; Sullivan, J ; Hofmann, O ; Ligeti, E ; Marto, JA et al.
Phosphoproteomic profiling of mouse primary HSPCs reveals new regulators of HSPC mobilization
BLOOD 128 : 11 pp. 1465-1474. , 10 p. (2016)
IF: 13,164
DOI: 10.1182/blood-2016-05-711424

Candidate's publications unrelated to the work discussed in this thesis

Horváth, V.B. ; Soltész-Katona, E. ; **Wisniewski, É**. ; Rajki, A. ; Halász, E. ; Enyedi, B. ; Hunyady, L. ; Tóth, A.D. ; Szanda, G. Optimization of the Heterologous Expression of the Cannabinoid Type-1 (CB1) Receptor.
FRONTIERS IN ENDOCRINOLOGY 12 Paper: 740913 , 12 p. (2021)
IF: 6,055
DOI: 10.3389/fendo.2021.740913

Szanda, G ; **Wisniewski, É** ; Rajki, A ; Spät, A. Mitochondrial cAMP exerts positive feedback on mitochondrial Ca(2+) uptake via the recruitment of Epac.
JOURNAL OF CELL SCIENCE 131 : 10 Paper: jcs215178 , 9 p. (2018)
IF: 4,517
DOI: 10.1242/jcs.215178

Korzeniowski, MK ; **Wisniewski, E** ; Baird, B ; Holowka, D ; Balla, T. Molecular anatomy of the early events in STIM1 activation; oligomerization or conformational change?
JOURNAL OF CELL SCIENCE 130 : 17 pp. 2821-2832. , 12 p. (2017)
IF:4,401
DOI: 10.1242/jcs.205583

Csepanyi-Komi, R ; **Wisniewski, E*** ; Bartos, B ; Levai, P ; Nemeth, T ; Balazs, B ; Kurz, AR ; Bierschenk, S ; Sperandio, M ; Ligeti, E. Rac GTPase Activating Protein ARHGAP25 Regulates Leukocyte Transendothelial Migration in Mice.
JOURNAL OF IMMUNOLOGY 197 : 7 pp. 2807-2815. , 9 p. (2016)
* Roland Csépányi-Kömi and Éva Wisniewski should be considered joint first authors.
IF: 4,856
DOI: 10.4049/jimmunol.1502342

Kim, YJ ; Guzman-Hernandez, ML ; **Wisniewski, E** ; Echeverria, N ; Balla, T. Phosphatidylinositol and phosphatidic acid transport between the ER and plasma membrane during PLC activation requires the Nir2 protein.
BIOCHEMICAL SOCIETY TRANSACTIONS 44 : 1 pp. 197-201. , 5 p. (2016)
IF: 2,765
DOI: 1,0.1042/BST20150187

Kim, YJ ; Guzman-Hernandez, M-L ; **Wisniewski, E** ; Balla, T. Phosphatidylinositol-Phosphatidic Acid Exchange by Nir2 at ER-PM Contact Sites Maintains Phosphoinositide Signaling Competence.
DEVELOPMENTAL CELL 33 : 5 pp. 549-561. , 13 p. (2015)

IF: 9,338

DOI: 10.1016/j.devcel.2015.04.028

Pagnamenta, AT ; Howard, MF ; **Wisniewski, E** ; Popitsch, N ; Knight, SJL ; Keays, DA ; Quaghebeur, G ; Cox, H ; Cox, P ; Balla, T et al. Germline recessive mutations in PI4KA are associated with perisylvian polymicrogyria, cerebellar hypoplasia and arthrogryposis. HUMAN MOLECULAR GENETICS 24 : 13 pp. 3732-3741. Paper: ddv117 , 10 p. (2015)

IF: 5,985

DOI: 10.1093/hmg/ddv117

Baumlova, A ; Chalupska, D ; Różycki, B ; Jovic, M ; **Wisniewski, E** ; Klima, M ; Dubankova, A ; Kloer, DP ; Nencka, R ; Balla, T et al. The crystal structure of the phosphatidylinositol 4-kinase IIα.

EMBO REPORTS 15 : 10 pp. 1085-1092. , 8 p. (2014)

IF: 9,055

DOI: 10.15252/embr.201438841

DOI:10.14753/SE.2023.2903

12. ACKNOWLEDGEMENTS

I would like to express my sincere gratitude to my supervisors, Professor Erzsébet Ligeti and Dr. Roland Csépányi-Kömi, who invited me to work at the Department of Physiology and have supported me ever since. I always could and still can count on them with any professional and personal matter. Their wisdom and wealth of experience have inspired me throughout my studies.

I am thankful to Dr. Tamás Balla, who welcomed me into his laboratory at the National Institutes of Health and taught me many techniques as well as scientific thinking during my one-year-long scholarship. I could not wish for a better start as a Ph.D. student.

I also wish to thank Professors László Hunyady and Attila Mócsai, heads of the Department of Physiology, and Prof. Péter Enyedi, chairman of the Molecular Medicine Doctoral School, for giving me the opportunity to pursue my Ph.D. and creating a friendly, supportive and inspiring atmosphere in the department. I am very grateful to Prof. András Spät for his professional support and friendship.

I am indebted to my colleagues in the Department of Physiology, who were always ready to help me. I could not imagine this journey without my immediate lab coworkers, Drs. Ferenc Kolonics, Ákos Lőrincz, Csaba Timár, Viktória Szeifert, Balázs Bartos, Domonkos Czárán, Péter Sasvári, Fanni Kovács and Enikő Bahurek who were always there to talk about research, teaching, studying or just to brainstorm. My experiments would not have been possible without the constant help of Regina Tóth-Kun, whose meticulous technical assistance, proactive and attentive personality made our work considerably easier and our time in the lab more enjoyable. I also wish to thank Dr. András Balla for his insightful suggestions regarding the bioluminescence resonance energy transfer experiments and Dr. Tamás Mészáros for helping us with the phosphoprotein staining.

Last but not least, I would like to express my appreciation to my family. Their unconditional love gave me strength and self-confidence when I needed the most. Finally, I would also like to give special thanks to Dr. Gergő Szanda, who helped me every step of the way.